VÄRMEFORSK

Effect of fuel quality on the bed agglomeration tendency in a biomass fired fluidised bed boiler

**Bengt-Johan Skrivfars, Maria Zevenhoven,
Rainer Backman, Marcus Öhman, Anders Nordin**

**DELPROGRAM
TILLÄMPAD FÖRBRÄNNINGSTEKNIK** **684**

Effect of fuel quality on the bed agglomeration tendency in a biomass fired fluidised bed boiler

Inverkan av bränslesammansättningen på bäddagglomereringstendensen i en svävbäddspanna vid förbränning av biomassa

Bengt-Johan Skrifvars, Maria Zevenhoven, Rainer Backman,
Åbo Akademi University, Process Chemistry Group

Marcus Öhman, Anders Nordin,
Energy Technology Center, Piteå

B8-803

VÄRMEFORSK Service AB
101 53 STOCKHOLM – TEL 08/677 25 80
Mars 2000
ISSN 0282-3772

Partners:
Åbo Akademi University, Process Chemistry Group, Åbo, Finland
Energy Technology Center, Piteå, Sweden
Brista Kraft, Sigtuna Energi, Rävsta, Märsta, Sweden
Skellefteå Kraft AB, Skellefteå, Sweden
Falun Energi, Falun, Sweden
Söderenergi, Södertälje, Sweden
C-4 Energi, Kristianstad, Sweden

Abstract

This report presents the results from a research project dealing with bed agglomeration problems in fluidised bed boilers firing forestry typed fuels. The project focused on how the bed agglomeration process proceeded in detail and on predicting the bed agglomeration temperature.

Five fuels were tested on their bed agglomeration tendency with a controlled bed agglomeration test, performed in an externally heated lab scale fluidized bed reactor. Bed samples were taken from the reactor during the test and analysed with SEM/EDS. Thermodynamic multicomponent multiphase equilibrium estimations were used for determining the stickiness of the bed samples.

The fuels were also analysed with a selective chemical leaching test on their ash forming elements in the fuel (Si, Al, Fe, Ca, Mg, P, Na, K, Cl, S). Based on these analyses, predictions were made on how the fuel would behave in a fluidized bed boiler with respect to bed agglomeration behavior.

The work showed that all five tested fuels seemed to have a fairly high tendency to form bed agglomerates when fired in a fluidized bed boiler with silica sand as bed material. In all the studied cases the bed agglomeration seemed to proceed according to three steps. Firstly a coating was formed on the bed particles, secondly the coating became sticky as the temperature in the bed was raised and thirdly the sticky coating started to attract other bed particles, causing agglomerates to form and finally causing de-fluidization. In all the studied cases the composition of the coating was fairly similar.

A correlation between the results from the selective chemical leaching test and the composition of the coatings was achieved when comparing the water and ammonium acetate leachable elements Ca, K and Na with the coating composition. These elements were always leached out from he fuel by water and ammonium acetate and always also found in the coatings. Sulfur and chlorine was also leached out in most of the cases but these two elements were not found in the coatings. The thermodynamic calculations suggest that these elements escaped the bed in a gaseous form, sulfur as sulfur dioxide (SO_2) and chlorine as potassium or sodium chloride (KCl or NaCl).

The practical implication from the results is that the fuel analysis is an essential part of a bed agglomeration prediction procedure but other aspects such as the furnace conditions and possible re-circulation processes of bed materials must also be included.

INVERKAN AV BRÄNSLESAMMANSÄTTNINGEN PÅ BÄDDAGGLO-MERERINGSTENDENSEN I EN SVÄVBÄDDSPANNA VID FÖRBRÄNNING AV BIOMASSA
SLUTRAPPORT

Bengt-Johan Skrifvars, Maria Zevenhoven, Rainer Backman,
Processkemiska forskargruppen, Åbo Akademi, Åbo, Finland

Marcus Öhman, Anders Nordin,
Energitekniskt Centrum, Piteå, Sverige

Svenskt sammandrag

Denhär rapporten presenterar resultat från projektet ”Inverkan av bränslesammansättningen på bäddagglomereringstendensen i en svävbäddspanna vid förbränning av biomassa”. I projektet fokuserade man på hur bäddagglomereringen framskrider i en sandbädd då man eldar biomassa samt på hur man kunde prediktera processen innan den sker.

Mera specifikt ville man utreda
- hur bäddmaterialet, speciellt sammansättningen på det skal som bildades på varje bäddpartikel vid förbränningen, varierade för olika bränslen
- om sammansättningen på skalet korrelerade med bränslets lättutslösliga askbildande element
- om det finns en korrelation mellan mängden kisel, uppbundet i bränslets organiska del och bäddagglomereringstendensen.

Fem bränslen inkluderades i studien, bark, brun grot, grön grot, returflis och sågavfall (spån). Alla fem bränslen genomgick följande delstudier, i) avanserad bränsleanalys, bestående av s.k. kemisk fraktionering, ii) kontrollerat bäddagglomereringstest i en lab-rigg, iii) SEM/EDS analys av bäddmaterialet från det kontrollerade bäddagglomereringstestet i labb-riggen, iv) estimering av bäddmaterialets smältbeteende och v) estimering med hjälp av termodynamisk jämviktskalkyl av varje bränsleaskas termiska beteende (komponent- och fassammansättning som funktion av temperaturen).

Resultaten från de kontrollerade bäddagglomereringstesten visade att alla fem testbränslen hade medelmåttig till hög tendens att bilda bäddagglomerat i en sandbädd. Alla bäddagglomererings-temperaturer låg mellan 930 och 980°C. Dessa uppmätta temperaturer stämmer väl överens med tidigare erfarenheter med liknande bränslen. Temperaturerna var klart lägre än motsvarande temperaturer för oproblematiska bränslen såsom vissa torv- och kolbränslen. För oproblematiska kol och torvbränslen har man uppmätt bäddagglomereringstemperaturer typiskt över 1000°C. För problematiska bränslen har man uppmätt bäddagglomereringstemperaturer under 850°C.

För de fem studerade fallen verkade bäddagglometreringsprocessen framskrida i tre steg. Först bildades ett skal på bäddpartiklarna, bestående av valda askbildande element från bränslet, främst kalcium (Ca) och kalium (K) samt av huvudelementet i bäddmaterialet, kisel (Si). Då sedan temperaturen höjdes i bädden externt, bildades en smälta i skalet som gjorde partikeln ”kladdig”. Då slutligen tillräkligt stor andel smälta bildats, fastnade bäddpartiklarna ihop i varandra, agglomererade, och förorsakade störningar i fluidiseringen.

I alla fem studerade fall hade bäddpartikelskalet i stort sett samma sammansättning trots att sammansättningen av de askbildande elementena i bränslet varierade. Skalets huvudelement var i alla situationer kisel (Si). Vidare fanns det alltid betydande mängder kalcium (Ca) och kalium (K) samt smärre mängder fosfor (P). I returflis-fallet hittade man också natrium (Na) i bäddpartikelskalet. Högst troligen befann sig Ca, K och Na i form av silikat i skalet medan P antagligen hade bildat kalciumfosfat.

Den praktiska indikationen från dessa resultat är att alla de studerade bränslena är mer eller mindre problematiska i en svävbädd då man använder sand som bäddmaterial. Bäddagglomereringen verkar också temperaturkänslig, vilket kan härledas från det faktum att det främst verkar finnas bäddpartiklar i bädden. Andelen aska (från bränslet) i bädden som enskilda partiklar verkar låg. Detta leder till att så fort bäddpartikelskalet blir ”kladdigt” uppträder agglomereringen mycket kraftigt. Askans ”buffrande” inverkan saknas. De upplevda skillnaderna i bäddagglomereringstendens som de olika anläggningarna rapporterat verkar alltså bero mera på pannspecifika parametrar såsom bäddtemperaturfluktuationer eller därtill relaterade effekter, snarare än bränslespecifika skillnader.

En korrelation mellan vissa lättutlösliga askbildande element i bränslet och bäddpartikelskalets sammansättning kunde skönjas. Kalcium, kalium och natrium löstes ut, i alla situationer de återfanns i bränslet, som lättlösliga element med vatten och/eller ammoniumacetat som lösningsmedel. Dessa element återfanns också i alla situationer i bäddpartikelskal.

Svavel och klor löstes också ut av vatten och ammoniumacetat . Dessa element återfanns dock inte i ett enda bäddpartikelskal i denna studie. Uppenbarligen binds dessa element inte upp i en kiselbaserad bädd utan passerar ut med rökgaserna som svaveldioxid- (SO_2) och alkalikloridgas (KCl, NaCl).

Resultaten från studien indikerar vidare att skalen på bäddpartiklarna bildas inåt mot bäddpartiklarnas centrum, men aldrig når centrum. Skaltillväxten verkar stoppa då skalet är ca 10μm tjockt. Kisel uppbundet i bränslets organiska del verkade inte påverka varken skalbildningen eller tendensen till bäddagglomeration.

Den praktiska implikationen av dessa resultat är att en noggrannare bränslekarakterisering än den standardmässiga analysen är viktig att utföra om man vill förutspå askrelaterade problem vid förbränning. Man måste dock ytterligare också beakta pannspecifika skillnader då dessa predikteringar görs.

Table of Contents

Abstract 2

Svenskt sammandrag 4

1. INTRODUCTION 7

2. GOAL 8

3. APPROACH 8

4. EXPERIMENTAL AND METHODS 9
- 4.1. Chemical fractionation analysis 9
- 4.2. Controlled fluidized bed agglomeration tests 10
- 4.3. SEM/EDS analyses of bed samples 11
- 4.4. Melting behavior estimations 11
- 4.5. Ash behavior predictions 12

5. RESULTS 12
- 5.1. Chemical fractionation analysis 12
- 5.2. Controlled fluidized bed agglomeration tests 14
- 5.3. SEM/EDS analyses of bed samples 14
- 5.4. Melting behavior estimations 15
- 5.5. Ash behavior predictions 16

6. DISCUSSION 18

7. CONCLUSIONS 21

Literature 23

APPENDIX, Figures 25

EFFECT OF FUEL QUALITY ON THE BED AGGLOMERATION TENDENCY IN A BIOMASS FIRED FLUIDISED BED BOILER FINAL REPORT

Bengt-Johan Skrifvars, Maria Zevenhoven, Rainer Backman,
Process Chemistry Group, Åbo Akademi University, Åbo, Finland

Marcus Öhman, Anders Nordin,
Energy Technology Center, Piteå, Sweden

1. INTRODUCTION

Bed agglomeration is a common reason for decreased availabilty of biomass fired fluidized bed boilers. Bed agglomeration disturbs the combustion process in the furnace and may in the worst case cause full defluidization of the bed which leads to an immediate shut down of the boiler. Of the five biomass fired fluidized bed boilers participating in this study three boilers reported serious bed agglomeration problems and all five reported some kind of bed disturbances during normal operation. One boiler reported 3 unsceduled shut downs for the last firing season due to bed agglomeration.

Common ways of fighting this problem are i) decreasing the bed temperature and ii) replacing the bed material. All five boilers in this study reported bed agglomeration problems when the average bed temperature exceeded some 890-900°C. All five reported also a more or less continuous replacing of bed material during high season operation. In two of the worst cases the whole bed was reported to be replaced in a couple of days.

Neither of these problem solving options are optimal since both lead to increased costs for the boiler operation, the former due to the derating of the boiler, the latter due to increased material costs.

Earlier studies have shown that the bed agglomeration process may be treated as a series of sequential steps as it proceeds /1-3/. Firstly the ash forming elements in the fuel are released from the fuel, secondly they are transported to the surface of the bed particles forming a coating on the bed particles and thirdly the coated bed particles stick together and form agglomerates.

The third step is the one where most knowledge is available today. Qualitative predictions of bed agglomeration temperatures can today already be made if the composition of the coating is available. These predictions are based on the assumption that the stickiness of the coating initiates the agglomeration process and that the stickiness is dependent on the presence of a molten phase in the coating. By estimating the melting behaviour of the coating with thermodynamic phase equilibrium studies one can extract agglomeration temperatures.

In fluidized bed biomass firing, where sand often is used as bed material, the coating has been found to consist of a mix of elements typically found both in the fuel as well as in the bed material /1, 3-6/. However, a clear segregation seems to take place for the ash forming elements in the fuel. Elements such as potassium and calcium seem to be caught very efficiently in the coating of a silicon based bed material while elements like chlorine and sulfur seem to escape a sand bed almost completely /1-3/.

The studies show also that silicon almost always is found in the coatings of sand bed particles from biomass firing /1-3/. Wether this silicon comes from the bed particle or from the fuel is not clear. It has, however, been hypothesized that a biomass that contain high amounts of silicon as an ash forming element would cause more bed agglomeration problems than such a biomass with a low amount of silicon /2, 3/.

It has also been hypothesized that such ash forming elements that would be easily released from a fuel during the combustion process would be more prone to adsorb on bed particle surfaces than others /7/.

2. GOAL

In this project we wanted to study the bed agglomeration process more in detail. We wanted to learn how the process proceeds in detail and how to predict the bed agglomeration temperature for a number of biomass fuels that would be interesting for heat and power producers.

More specifically the goals could be broken down into the following working hypothesis:

1) How did the coating of a sand bed material vary when different biomass fuels were fired in an FBC. Here we wanted to track down both qualitatively and quantitatively where the elements in the coating would come from and compare our bed behavior predictions with full-scale operational experiences where available.

2) Would there be a correlation between easily released ash forming elements in the fuel and the composition of the coating of a sand bed. If this would be the case we would be able to make predictions on bed agglomeration tendencies based on advanced fuel analyses.

3) Would a biomass that contains high amounts of silicon tied up in its organic part cause more bed agglomeration problems than a biomass with a low amount of silicon.

3. APPROACH

The work was divided into four parts, i) advanced fuel analyses, so called chemical fractionation analyses, ii) controlled bed agglomeration tests in an FBC lab rig, iii)

scanning electron microscopy studies of bed agglomerates from the test rig and iv) thermodynamic phase equilibrium studies.

With the chemical fractionation analyses we wanted to quantify how ash-forming elements were bound to the fuels that were studied and to see if these data could be directly used for extracting data on which elements would be easily released from a fuel and which don't. We wanted also to make bed agglomeration predictions directly based on the chemical fractionation analysis results.

With the controlled bed agglomeration tests we wanted both to characterize the bed agglomeration tendencies for the fuels to be studied, as well as to collect bed materials for further analyses of the bed particle coatings.

With the scanning electron microscopy studies of bed agglomerates from the test rig we wanted to detect what the elements in the coatings were and how they varied depending on the fuel.

The thermodynamic phase equilibrium studies were used in two separate ways. Firstly they were used for estimating the melting behavior of the coatings. This was done both by extracting phase behavior data from available 3-phase diagram as well as by using existing thermodynamic data to calculate the melting behavior. Secondly the phase equilibrium studies were used for predicting the melting behavior of assumed ash particle fractions where the assumptions were based on the chemical fractionation results.

4. EXPERIMENTAL AND METHODS

Five fuels were selected to the study, bark (bark), forest residue type 1 (brun grot), forest residue type 2 (grön grot), sawdust (sågspån), and construction residue wood (returflis),. All five fuels were used in the four different parts of the project as described below.

The fuels included in the study were selected partly so that they would represent the interests of the participating energy producers, partly to represent a variety of forestry based fuels with as much variations in combustion behavior experience as possible.

4.1. Chemical fractionation analysis {TC "1.1. Chemical fractionation and analysis " \l 2}

Chemical fractionation of the five solid fuels was carried out according to literature /8, 9/.

The analysing technique distinguishes different types of ash forming elements in the fuel according to their solubility in different solvents. Increasingly aggressive solvents, *i.e.* water (H_2O), 1N ammonium acetate (NH_4Ac) and 1N hydrochloric acid (HCl) leaches samples into a series of four liquid and solid samples. Both solid and liquid samples are then analysed for Si, Al, Ti, Fe, Ca, Mg, Na, K, S, P, and Cl.

Typical ash forming elements, which leach out by water are sodium (Na), potassium (K), sulfur (S) and chlorine (Cl) in mixed compounds of alkali sulfates, carbonates and chlorides. Elements leached out by ammonium acetate are believed to be ion exchangeable elements, associated organically in the fuel. These elements may be sulphur, calcium, potassium and sodium. The hydrochloric acid leaches out the carbonates and sulphates of earth alkali elements and iron. Silicates and other minerals usually remain in the insoluble rest. A schematic view of the method is presented in Figure 1.

Based on the chemical fractionation analysis we then divided the ash forming elements into two parts, a "mobile part" and an "immobile part". The mobile part consisted of those ash-forming elements that were leached out by water and ammonium acetate while the immobile part consisted of those elements leached out by HCl and those not being leached out at all.

The reasoning behind this division was the assumption that those elements that would be easily leached out from the fuel, i.e., by water and acetate, would also be easily released from the fuel during a combustion process and form gases or sub-micron sized particles. Consequently they would be relatively reactive and "mobile" and could for example escape the bed and cyclone and end up in the fluegas channel as fly ash or deposits. This trend has actually been shown earlier /10, 11/.

The elements being leached out by the HCl solution and those elements staying in the rest fraction would again be in a less mobile part. Usually these elements are found in mineral grains in the fuel or as contaminations associated with the fuel but not directly tied up in the fuel.

These two parts, i.e., the mobile and the immobile part, we will use in the further text when we refer to the chemical fractionation results and ash behaviour predictions.

4.2. Controlled fluidized bed agglomeration tests

The controlled fluidized bed agglomeration method has previously been described in the literature /12/ and only a brief description is given here. The bench-scale reactor (5 kW) (see Figure 2), is constructed from stainless steel, being 2 m high, 100 mm and 200 mm in bed and freeboard diameters, respectively. To obtain isothermal conditions in the bed, and to minimize the significant influence of cold walls in such a small-scale unit, the reactor is equipped with electrical wall heating elements, equalizing the wall and bed temperatures.

The agglomeration tests were initiated by loading of the bed with a certain ash to bed material ratio, under normal FBC conditions. The excess oxygen concentration was controlled to 6 % (wet gases). A fluidization velocity of four times the minimum fluidization velocity was used, and the bed temperature was maintained at 800°C for all fuels. At an ash amount corresponding to approximately 6 wt-% ash in the bed, the fuel feeding was stopped and the operation was switched to external heating.

The bed was then heated up, at a rate of 3 ^{o}C/min, to the point where it agglomerated. To maintain a combustion atmosphere in the bed during the external heating phase, propane was mixed with the primary air in a chamber prior to the air distributor.

The onset of bed agglomeration was determined by monitoring differential pressures and temperatures in the bed. The detection of initial bed particle cohesion was facilitated by on-line principal component analysis, PCA, by considering all bed-related variables (3 temperatures and 4 differential pressures) simultaneously. The principles of using PCA in determining the bed agglomeration temperature like it was used here, are presented in the literature /2/. A typical illustration of fluctuations in temperatures and differential bed pressures versus time in a controlled bed agglomeration test run is shown in Figure 3. The final de-fluidization can clearly be seen here as a drop in the bed pressure.

Earlier studies /12/ have shown that only 1.5 % of ash in the bed is sufficient for agglomeration to occur and no significant influence on the determined agglomeration temperature by the variables “amount of bed material”, “heating rate”, “fluidization velocity” or “air-to-fuel ratio” has been found.

4.3. SEM/EDS analyses of bed samples

Throughout the experimental runs, samples of the bed material were collected using an air-cooled suction probe, equipped with a cyclone separator. Three samples were taken for each run, one sample at the end of the combustion period, another sample in the bed temperature increase phase and a third bed samples at the agglomeration temperature. Of these three samples the actual bed agglomerate sample at the end of each run was analyzed with SEM/EDS.

The samples were prepared by mounting them in epoxy, cut with a diamond saw and polished. The resulting cross-section area was then the goal for the examination. The examination consisted of three parts. For each sample a SEM micrograph was taken. The image was then analyzed with EDS on any element found in the sample. This was done using a mapping technique where the distribution of each analyzed element was mapped in the sample. As a final step a number of spot analyses were taken from selected points in the sample, such as agglomeration necks between particles and coatings of particles

4.4. Melting behavior estimations

Based on the semi-quantitative SEM/EDS analyses of coatings on the bed particles, the melting behavior of the coating material was estimated by i) extracting phase behavior data from phase diagrams and ii) by thermodynamic multi-component, multi-phase equilibrium calculations. The resulting melting behavior was then compared with the determined fuel specific bed agglomeration temperature.

<u>Estimations based on 3-phase diagrams</u>

When estimating the melting behavior of the coatings from experimentally determined 3-phase diagrams, all coating compositions were firstly normalized to the three major elements. In this case all coating analyses of all samples, regardless of fuel, were normalized to the 3-phase system “calcium (Ca) - potassium (K) - silicon (Si)”. In all cases

except for the construction reject wood, these three elements represented almost 90 % of the elements analyzed in the bed particle coatings. For the construction reject wood also sodium was present. But since potassium and sodium generally are assumed to behave similarly in chemical systems, we neglected the presence of sodium.

The actual melting behavior estimations were then performed according to well established procedures, using the "lever rule" as the main tool, and reading the amount of melt with 50°C intervals. Each analyzed coating point resulted in a melting vs. temperature curve.

Estimations based on phase equilibrium calculations

A similar melting-vs-temperature curve was also produced by using thermodynamic multi-component, multi-phase equilibrium calculations. This procedure is based on Gibbs' free energy minimisation and has the possibility to take into account multi-component and multi-phase systems. The key knowledge to these calculations is the thermodynamic data used in the calculation procedure. Here we used data partly from own developments /13-15/, partly taken from the literature /16-19/. The database included data for 14 elements, 120 gaseous components, two liquid phases (a salt melt and an oxide melt), 12 solid solution phases and 73 pure condensed phases and has been succesfully used at several occasions before /20-22/.

The melting behavior calculations were done using the average coating composition of the analyzed bed samples. Each composition resulted in one melting curve.

4.5. Ash behavior predictions

As a separate part we also made predictions of the bed agglomeration temperature using the thermodynamic phase equilibrium calculations.

We based the predictions on the chemical fractionation analysis of the fuel in such a way that we estimated the thermal behavior of the mobile and immobile part separately. In both calculations the fuel related carbon, nitrogen and oxygen were assumed to be the same as in Scandinavian softwood, corrected with the ash amounts as analysed in the fractionation analyses. In the calculations an atmospheric combustion case was modelled using an air factor of 1.2 and atmospheric pressure of 1 bar. The calculations were carried out for a temperature range 500-1200°C.

For all five fuels the calculations resulted in graphs showing the distribution of the stable condensed phases (liquid and solid) as a function of temperature for both the mobile as well as the immobile part.

When interpreting the results of these calculations their limitations should be recognised. The equilibrium approach implies that no reaction kinetics nor fluid dynamic effects are taken into account. Nevertheless an interpretation of the results may give useful information about the studied system.

5. RESULTS

5.1. Chemical fractionation analyses {TC "1.1. Chemical fractionation and analysis " \l 2}

Results from the fractionation of the different fuels are shown in Figures 4a through 8b. The figures "a" show the amounts of silicon (Si), aluminium (Al), iron (Fe), titanium (Ti), calcium (Ca), magnesium (Mg), sodium (Na), potassium (K), sulfur (S), phosphour (P), and chlorine (Cl) in the leachates expressed as g/kg dry fuel. Crosses show the amount of the specified elements present in the untreated fuels. A clear bar represents the amount of ash forming elements leached out by water. A striped bar the amount of ash forming elements by the acetate and a grey bar by the HCl. A black bar represents the amount of ash forming elements not leached out by any of the leaching agents. Figures "b" show the distribution of a certain element over different leaching phases. Thus, in the ideal case the sum of calculated percentages should be 100%.

The amounts of leached elements were determined both from the solid and from the liquid analyses. The leached amounts of ash forming elements could be taken directly from the liquid analysis. From the solid analysis it had to be calculated by subtracting the amount of element found in the solid fraction after leaching from the amount before leaching etc. It should be noted here that the sum of all fractions, i.e., H_2O, NH_4Ac, HCl and rest fraction, not always was the same as the amount as determined in the untreated solid. There was a rather big discrepancy between solid and liquid analysis. In the cases considered here the liquid analysis is supposed to be more trustworthy than the solid analysis. Therefore only the results of the liquid analysis will be described hereafter.

The analysis results will be qualitatively described fuel by fuel in the text below.

Bark {TC "Bark " \l 3}

The total content of ash forming elements in bark was rather high i.e. some 30 g/kg dry fuel. This corresponds to some 5.5 w-% of ash. The bark as shown in Figure 4 and b contained much silica some 12 g/kg fuel. The two other main ash-forming elements were calcium and potassium.

The main part of silica and also aluminium and iron was found in the rest fraction. This indicated a high presence of minerals, probably soil contamination in the fuel.

Both calcium and magnesium were merely present in the water and acetate fraction only some 20% of the total amount present could be found in the HCl and rest fraction. Up to 90% of the sodium was found in the HCl and rest fraction, whereas about half of the potassium was found in the water-acetate fractions. Almost all sulfur was found in the HCl and rest fractions. Chlorine was found in the water fraction.

Forest residue, type 1 (Brun grot) and type 2 (Grön grot) {TC "Brun and grön grot " \l 3}

Figures 5a through 6b show the results for forest residue type 1 and type 2. When compared with bark it is shown clearly that both types have a much lower content of ash forming elements in the fuel. For the Forest residue type 1 the total amount was 11 g/kg dry fuel, corresponding to some 2 w-% ash and for the Forest residue type 2 the numbers

were 13 g/kg db corresponding to 2.8 w-% ash. The main ash forming elements in these two types of forest residue were silica, calcium, magnesium, and potassium.

For the Forest residue type 2 the main part of the silica, aluminium and iron was present in the rest and HCl-fraction. In the Forest residue type 1 a significant amount of silicon was found also in the acetate fraction. Calcium and magnesium were found in all fractions. The calcium was divided more or less evenly over the water-acetate and HCl-rest fractions, while the major part of magnesium was found in the water and acetate fraction. In the forest residue type 1 (Brun grot) about 40% of sodium was found in the rest fraction, whereas this was up to 70% in the type 2 (Grön grot). In both types the major part of potassium was found in the water and acetate fractions. The major part of sulfur was found in the HCl and rest fractions.

Construction residue wood{TC "Returflis " \l 3}
This fuel had the highest amount of ash forming elements in it, i.e. some 40 g/kg dry fuel corresponding to 7 w-% ash. Figures 7a and b show that the main ash-forming element in the fuel was silicon, followed by calcium, iron, and aluminium. Titanium was also detected, apparently present as small amounts of paint residue on the wood.

Silica was found in the HCl and rest fractions. About half of the aluminium was found in the rest fraction. The other half was found in the HCl fraction. The major part of calcium (some 60%) was found in the acetate and water fractions whereas in the case of magnesium this was only some 25%. About 20-30% of the sodium and potassium was present in the water fraction, the rest in the HCl and rest fractions. The main part of sulphur was found in the acetate and water fraction. Chlorine was believed to be leached out of the fuel in the water step completely.

Sawdust{TC "Sågavfall " \l 3}
Sawdust as shown in Figures 8a and b contained the lowest amount of ash forming elements, i.e. 4 g/kg in dry fuel corresponding to some 0,7 w-% ash. The ash was relatively high in silica, calcium and potassium.

In this fuel the silica seemed further to be present both in the acetate fraction as well as in the rest. Calcium and magnesium were present mainly in the water and acetate fractions whereas the main part of potassium was present in the water fraction. Some 70% of the sulphur was found in the HCl and rest fraction whereas this was some 50% for the phosphor. Again chlorine was found in the water fraction.

5.2. Controlled fluidized bed agglomeration tests

The controlled agglomeration tests of the different fuels resulted in agglomeration temperatures of 930 to 980°C. These results are presented in Figure 9.

The lowest T_{aggl}, some 930°C, was found for Bark and the Forest residue type 1 (Brun grot). Sawdust followed with a T_{aggl} of approximately 940°C and Construction residue wood with T_{aggl} of 950°C. The highest T_{aggl} was found for the Forest residue type 2 (Grön grot). Here the T_{aggl} temperature was found to be 980°C.

5.3. SEM/EDS analyses of bed samples

Figures 10 and 11 show a typical SEM/EDS analysis of a bed agglomerate sample from the sawdust firing case. Figure 10 consists of a so-called back-scatter image of a number of bed particles, fixed in epoxy resin and cross-sectioned. The dark area in the image is the epoxy resin and the lighter areas are the cross-sectioned bed particles. A shift in the grey tone of the particle indicates a shift in elemental composition of the area. A lighter one indicates heavier elements present in the analyzed area, such as Fe, Al, or Si, while a darker one indicates lighter elements such as Na, K, and Ca. As can be seen, all bed particles are coated with a material, different from the pure bed material. The coating is some 10 μm thick.

Figure 11 presents an elemental map of the bed sample shown in Figure 10, where the distribution of the elements Na, Mg, Al, S, Cl, Ti, Fe, Si, P, Ca and K is shown. A light area indicates a higher concentration of the element in question than a dark area. Looking at these maps one can see that the cores of the bed particles always consist of almost pure silicon (Si) while the coatings contain also other elements. The same trend could be found in all analyzed samples, independently of fuel.

Figure 12 summarizes the spot analyses made on coatings of the bed particles in each run. The figure clearly shows that the coatings of all bed samples except for the construction residue wood case, contain silicon, calcium and potassium as major elements. Phosphor is also usually found in the coatings but to a clearly lower extent than calcium or potassium.

For the construction residue wood case the potassium is exchanged to sodium in the coating and instead of phosphor, iron may be found in the coating

5.4. Melting behavior estimations

Figure 13 shows the K_2O-CaO-SiO_2 ternary diagram /23/. In this diagram the average compositions (20-40 spot analyses) of the bed material coatings from the controlled bed agglomeration tests of the five studied fuels have been included as plot marks. As can be seen the compositions are mainly restricted to the SiO_2 rich corner in the phase diagram. Silicates with these compositions have a first melting temperature of 720°C, while a small addition of calcium will shift this value to roughly 1080°C.

The melting behavior evaluations were then done by extracting melting behavior data from the phase diagram. Only coatings that had elemental compositions (>90 %) within the ternary diagram in Figure 13 were included in the comparison. The resulting fractions of melt (solid lines) versus temperature are shown in Figure 14 together with the determined initial agglomeration temperature (vertical broken line), determined by the controlled bed agglomeration test. The agglomeration temperatures from the lab tests agree fairly well with the temperatures at which the melting behavior evaluations indicate a high fraction of melt in the coating.

The melting behavior of the coatings was also estimated with thermodynamic multi-component, multiphase equilibrium calculations. Here the estimation was based on the

average compositions of the coatings (the plot marks in Figure 13). These results are also shown in Figure 14 as the thick dotted curves in each plot.

5.5. Ash behavior predictions

As described in chapter 4.5, we also used the thermodynamic calculations, combined with the chemical fractionation analyses, to predict the bed agglomeration tendency for each fuel. Important parameters we looked for when predicting the bed agglomeration were the first melting point of the calculated ash fractions and the maximum amount of molten phase present in the calculated temperature range.

The results are summarised in Table 1 and in the Figures 15 - 19. Table 1 presents the numbers for the first melting temperature and the maximum amount of melt, calculated for the mobile and immobile ash fractions of each fuel. The figures show the whole melting behavior curve for both ash fractions in the calculated temperature range 500 – 1200°C as well as the compositions of the solid and liquid phases in both ash fractions.

Table 1: *The first melting point, T_0, and the maximum amount of melt at a certain temperature as calculated for the 5 fuels in the temperature range 500-1200°C.*

	Mobile part		**Immobile part**	
	First melting Temperature , T_0 (°C)	Max. amount of molten phase (w-% @ °C)	First melting temperature, T_0 (°C)	Max. amount of molten phase, (w-% @ °C)
Bark	825	9 @ 875	925	60 @ 1200
For. Res. Type 1	600	51 @ 825	825	48 @ 1200
For. Res. Type 2	> 1200	0 @ 1200	725	57 @ 1200
Constr. Res	500	3 @ 650	850	62 @ 1200
Saw dust	750	36 @ 800	1050	37 @ 1200

Bark (Figure 15){TC "Bark " \l 3}

The calculations indicate that the main components of the mobile ash fraction of bark would be potassium carbonate, magnesium oxide and calcium carbonates in the lower temperature range. Also a small amount of sodium carbonate is interpreted to form. In a higher temperature range calcium carbonate would decompose to calcium oxide and the potassium and sodium carbonate would melt at some 825°C, forming a molten phase of potassium and sodium carbonate. This liquid is estimated to be at its maximum value of 9 wt-% at 850°C. After this it is calculated to evaporate in the temperature region of 850°C – 925°C and has disappeared completely at temperatures above 925°C. In the whole temperature range, solid calcium phosphate and forsterite (magnesium-, calcium silicate) were calculated to be stable and at temperatures below 600°C a small amount of solid potassium chloride to be present. At temperatures above 625°C potassium chloride would evaporate.

The main components in the immobile ash fraction were calculated to be different types of silicates, which could form a glassy melt at temperatures above 925°C together with sodium, potassium and aluminium. The liquid silicate melt was estimated to increase up to

the maximum calculated temperature of 1200°C where it was estimated to be some 60 wt-% of the total condensed phases (liquid + solid). Iron oxide, calcium phosphate and minerals such as cordierite, anorthite albite, and leucite were calculated to be present in the whole considered temperature range. Solid calcium sulphate was estimated to be present at temperatures below some 800°C

Forest residue, type 1 (Figure 16, Brun grot){TC "Brun grot " \l 3}
The main components of the mobile ash fraction in the type-1 Forest residue was calculated to be solid sodium and potassium carbonate, with a first melting point of some 600°C. Potassium chloride was calculated to be present in a condensed form (solid or liquid) up to at some 700°C. At higher temperatures potassium chloride was calculated to evaporate. A glassy silica melt, containing sodium potassium, calcium and magnesium, was calculated to form above 650°C. Solid forsterite and calcium phosphate was again calculated to be present in the whole temperature range considered.

The main components in the immobile ash fraction was calculated to be wollastonite, iron oxide, calcium phosphate and anorthite, present in the whole temperature range. Calcium sulphate, albite and leucite was calculated to disappear at some 850°C, at which a silica rich glassy melt would form. This melt was calculated to consist of magnesium, calcium, aluminium. potassium, and sodium, besides silica.

Forest residue, type 2 (Figure 17, Grön grot) {TC "Grön grot " \l 3}
The mobile ash fraction of the type 2 forest residue ("grön grot") was calculated not to form any molten phase. The major components of the solid phase were calculated to be potassium carbonate, potassium sulphate, potassium chloride, magnesium oxide, calcium carbonate and calcium phosphate. Potassium carbonate, was calculated to decompose at some 925°C, potassium sulphate, to decompose at some 1025°C, and potassium chloride to evaporate at some 650°C. Magnesium oxide and calcium phosphate was calculated to be present in the whole temperature range, whereas calcium carbonate decomposed at some 800°C forming a calcium silicate instead.

The immobile ash fraction was calculated to contain a molten silica phase at temperatures above 725°C. This phase was rich in calcium, aluminium, potassium an sodium. The solid phase was calculated to contain wollastonite, iron oxide, calcium phosphate, anorthite and leucite in the whole temperature range and calcium sulphate and albite at temperatures below 850°C.

Construction residue (Figure 18){TC "Returflis " \l 3}
The mobile ash fraction of construction residue was estimated to contain a molten phase already at a fairly low temperature. The first melting point was calculated to 500°C. Th composition of the molten phase was calculated to contain potassium- and sodium sulphates and -chlorides. The main component in the solid phase was calcium carbonate decomposing to calcium oxide at temperatures above 775°C. Other solid components, calculated to be present, were magnesium oxide, forsterite, calcium phosphate, calcium sulphate and iron oxide.

The immobile ash fraction was calculated to form a molten glassy phase at a temperature above some 850°C. This phase contained silica, potassium, sodium and aluminium. The main solid phases were calculated to be anorthite, albite (dissappearing at temperatures above 995°C), cordierite (appearing above 995°C), leucite and some small amounts of calcium phosphate, calcium sulphate and diopside.

Sawdust (Figure 19){TC "Sågavfall " \l 3}
The mobile ash fraction of sawdust was calculated to melt at some 750°C forming a molten phase of sodium carbonate, -sulphate and potassium carbonate, which was estimated to decompose and partly evaporate at some 1000°C. The solid phases consisted mainly of sodium- and potassium carbonate below 800°C, and magnesium oxide, forsterite, calcium phosphate and calcium silicate throughout the calculated temperature region.

The immobile ash fraction was calculated to form a glassy silica melt at a temperature above 1050°C. It was estimated to contain magnesium, calcium, aluminium, sodium and potassium besides silica. The solid phases consisted of mainly leucite, nepheline, anorthite calcium phosphate and - sulphate (below 825°C), iron oxide wollastonite and forsterite.

6. DISCUSSION

One of the main goals of this project was to study the bed agglomeration process more in detail for various biomass fuels. We defined also three more specific working hypotheses to be tested. In the following chapter these three hypotheses will be discussed based on the results obtained in the project.

The fuels and their bed agglomeration tendencies
The fuel analyses showed differences between the fuels with respect to their ash forming elements. Figure 20 shows the amount of the ash forming elements found in the mobile and immobile parts of each studied fuel. The total amount of ash forming elements, analyzed separately as the fuel ash, is shown as a cross at each bar. The amount of ash-forming elements, analyzed with the chemical fractionation technique, varied from 40 g/kg db ash forming elements in the construction residue to 4 g/kg db in the saw dust. These numbers correspond to some 6 w-% and 0,6 w-% ash respectively. The distribution of ash forming elements between the mobile and immobile part varied also. Construction residue and Bark had a major part of their ash forming elements in the immobile part while both the Forest residues and the sawdust had a more even distribution between the two parts. This indicates that Bark and Construction residue would have a higher total ash load to the boiler and most likely a higher bed ash inventory than in the case for the Forest residues and the sawdust.

Only small variations in the compositional distribution in the different fractions of the fuels could be found. The main trends were that calcium (Ca), magnesium (Mg) sodium, potassium (K), sulfur (S), phosphorus (P) and chlorine (Cl) always were found in the water and acetate fractions while silicon (Si), aluminum (Al) and iron (Fe) were found mainly in

the HCl and rest fractions. Only in two cases was the Si found in the water and acetate fractions, namely for the Forest residue type 1 and in the Saw dust.

The expected differences between the two forest residue types, 1 and 2, that type 2 would have had more ash forming elements in its mobile part than type 1, did not show up in the analyses. The analyses seem rather to suggest the opposite and the elemental distribution seems even to compare surprisingly well with the sawdust.

Construction residue wood was supposed to be rather incomparable with the other 4 fuels, since this was supposed to be a waste fuel, which could contain all kinds of unexpected contaminations. This was however, not the case. It compared well with the other test fuels and no major difference could be seen.

The bed agglomeration temperatures, T_{aggl}, detected either by the controlled bed agglomeration lab scale test or the theoretically predicted melting behavior calculation, revealed, however, no big differences. All T_{aggl}:s were in a relevant temperature range and detected to be fairly low, compared to other unproblematic fuels, which are fired in fluidized beds. Earlier experiences with these two detection methods, have shown that fuels like well behaving coals have T_{aggl}:s above 1000°C while very problematic ones have T_{aggl}:s below 800°C. Forestry typed and wood based fuels have typically had T_{aggl}:s around 850-1000°C.

It seems, however, that the differences found in the fuel analyses are not reflected in any direct way in the detected bed agglomeration temperatures. The clearest indication from these results is that forestry typed and wood based fuels are generally more or less problematic from a bed-agglomeration point of view, if silica sand is used as the bed material. It seems also clear that the bed agglomeration tendency is very temperature sensitive. This seems to be in accordance with the experiences from the full-scale boilers.

<u>The bed agglomeration process</u>
The SEM/EDS analyses indicate that the bed agglomeration proceeded as follows.

i) Firstly a coating was formed on the bed particles.
ii) Secondly the coating obviously became sticky as the temperature in the bed was raised.
iii) Thirdly the sticky coating started to attract other bed particles, causing agglomerates to form and finally causing de-fluidization.

It is obvious that this stepwise behavior may change if other fuels than those tested here are used.

<u>How did the coating of a sand bed material vary when different biomasses were fired.</u>
It was noted that the coating was some 1 – 10 μm thick in all cases. The thickness seemed to be somewhat dependent on the retention time of the bed particle in the bed, however not strongly. This can be seen when comparing the coating thicknesses from the saw dust with the other tests. Saw dust contained so low amount of ash forming elements that we had to

combust it for a longer time than the other fuels to reach a constant ash-to-bed ratio in the controlled bed agglomeration test. However, not in any of the tested cases could there be found coatings that would have been thicker than 10 μm.

The coatings were surprisingly similar in composition regardless of fuel. Only small differences in the compositions could be found even if the fuel analyses revealed differences between the fuels. Obviously the differences in the amounts of ash forming elements entering the bed with the various fuels were small enough so that the bed was able to even out them. This indication is also supported by the fact the detected bed agglomeration temperatures did not vary very significantly.

Would it be possible to make predictions on bed agglomeration tendencies based mainly on fuel data.

This hypothesis was based on the following reasoning. If there would be a correlation between easily released ash forming elements in the fuel and the composition of the coating of a sand bed, it should be possible to analyze the fuel on its content of these elements and then use this data to predict the bed agglomeration tendency.

Unfortunately the data do not give any direct correlation between the mobile part of the ash forming elements in the fuel, i.e., possible easily released ash forming elements, and the coating composition of the bed particles. Some trends can be seen such as the one that calcium, magnesium, potassium and sodium is found in both the coatings of the bed particles and the mobile part of the ash forming elements in the fuel. But the trends are not consistent for all the elements found in the mobile part. This concerns especially chlorine and sulfur, which both were found in the mobile part but never detected in the coatings on the bed particles. It seems clear that the furnace conditions also affect the formation of the coating very strongly.

An attempt was made to estimate how much of the main elements, found in the coating, could generate from the easily volatilized ash part in the fuel. The estimation was done for calcium (Ca), potassium (K) and silicon (Si), using the chemical fractionation analyses results and the SEM/EDS analyses of the coatings. Since we knew the amount of fuel and bed as well as the composition of the coating we could estimate how much of a certain element retained in the bed. A value above 100 w-% indicates that more of the element is found in the coating than would be found in the easily volatilized part of the fuel (the water and acetate fractions in the fractionation analysis).

For both Ca and K the estimations showed that there would be enough of them in the fuel and even in the easily volatilized part of the fuel to cover all Ca and K analyzed in the bed particle coatings. These estimations are presented in Figure 21, the two upper graphs. The lower graph shows a similar estimation for silicon (Si).

Would silicon tied up in the organic part of a biomass promote bed agglomeration problems

This hypothesis generated from the findings that i) silicon always seemed to be present in the coatings of silicate bed particles together with other ash forming elements from the fuel and ii) the coating seemed never to grow in thickness more than up to 10 μm.

Two options could be possible to achieve this kind of coating. The coating could either grow outwards on the bed particle or inwards into the bed particle. In the first option the elements found in the coating should have come from the fuel. After a certain time the growth would have stopped because of erosion in the bed.

In the second option certain elements should react with the bed particle (in this case mainly Ca and K). At some point the reaction stops due to some controlling step in the reaction, such as the diffusion of the reacting element through the formed coating into the reacting zone in the particle. This could explain why the observed thicknesses never exceed a certain value.

The first option does not seem to be supported by the results from this study. In only two of the studied cases we found Si in the easily volatilized fractions of the fuel analyses, but all bed particles showed Si in their coatings. As described earlier we also estimated if there would be enough silicon in the easily volatilized part in the fuel to cover the Si in the coatings, and we found that this was not the case. This is shown in the lower graph of Figure 20. As can be seen, the value of 100 % is significantly exceeded in most of the cases. This indicates that there always was estimated more silicon in the coatings than what was found in the fuel. The only exception to this was the Forest residue type 1 firing case.

The total amount of Si in the fuel would have been enough to cover the Si in the coatings but since we know that most of that Si probably was soil, we don't think it can transfer to the coatings. Concequently, the Si most likely came from the bed particle, which further indicates the option two for the coating formation mechanism.

7. CONCLUSIONS

This work showed that all five tested fuels seemed to have a fairly high tendency to form bed agglomerates when fired in a fluidized bed boiler with silica sand as bed material. The detected agglomeration temperatures varied in a fairly narrow temperature range from 930°C to 980°C. These temperatures are well in line with earlier experiences of firing forestry-typed fuels. The temperatures are also clearly lower than what has been experienced with typical unproblematic fuels such as peat or various types of coals. Here the T_{aggl}:s are typically above 1000°C.

For the fuels studied in this project the bed agglomeration seemed to proceed according to three steps. Firstly a coating was formed on the bed particles, secondly the coating became sticky as the temperature in the bed was raised and thirdly the sticky coating started to

attract other bed particles, causing agglomerates to form and finally causing de-fluidization.

In all the studied cases the composition of the coating was fairly similar. silicon (Si), calcium (Ca), and potassium (K) was always found in the coating of the bed particles for all fuels, as well as minor amounts of phosphorus (P). The coatings of the bed particles from construction residue firing contained sodium (Na) instead of phosphorus (P). Most likely Ca, K and Na were tied uo with silicon in a silicate phase in the coating, while P may have formed calcium phosphate.

The practical indication from this is that all the tested fuels are more or less identically problematic with sand bed and that the bed agglomeration process is very temperature sensitive. The experienced differences in boiler operation can with these fuels therefore probably not be explained with only fuel specific ash related data, but rather with sudden uncontrolled temperature fluctuations in the bed.

A correlation between the chemical fractionation analysis results and the composition of the coatings was achieved when comparing the water and ammonium acetate leachable elements Ca, K and Na with the coating composition. These elements were always leached out from he fuel by water and ammonium acetate and always also found in the coatings. sulphur and chlorine was also leached out in most of the cases but these two elements were not found in the coatings. The thermodynamic calculations suggested that these elements escaped the bed in a gaseous form, sulphur as sulphur dioxide (SO_2) and chlorine as potassium or sodium chloride (KCl or NaCl).

The results indicate for these fuels that the bed particle coating grows inwards to the center of the particle but never reaches the 100 % conversion. Instead the reaction stops at a fairly low conversion grade. Fuels with Silicon in their easily volatilized part, did not seem to be more prone to cause bed agglomeration than other fuels.

The practical implication from these results is that a fuel analysis is an essential part when bed agglomeration is predicted. However, other aspects such as the furnace conditions and possible re-circulation processes of bed materials must also be included.

LITERATURE

1. Skrifvars, B-J., Backman, R., Hupa, M.: "Ash chemistry and behavior in fluidized bed combustion – and overview", *in* LIEKKI 2 Combustion and gasification research programme, technical review 1993-1998, (Ed:s Hupa, M., Matinlinna, J.), Vol 1, p. 609, Åbo Akademis Tryckeri, Åbo, Finland 1998.
2. Öhman, M., "Experimental studies on bed agglomeration during fluidized bed combustion of biomass fuels", Dr. Thesis, University of Umeå, 1999.
3. Öhman, M., Nordin, A., Skrifvars, B-J., Backman, R., Hupa, M.: "Bed agglomeration characteristics during fluidized bed combustion of biomass fuels", *accepted 1999 for publication in Energy & Fuels.*
4. Skrifvars, B.-J., Sfiris, G., Backman, R., Widegren-Dafgård, K, Hupa, M., Ash Behavior in a CFB Boiler during Combustion of Salix, Energy and Fuel 11 (1997) 4: 843-848.
5. Latva-Somppi, J.; Kurkela, J.; Tapper, U.;Kauppinen, E. I.; Jokiniemi, J. K.; Johanson, B. *Proc. of* the International Conference on Ash Behavior Control in Energy Conversion Systems, 1998, 119-126, Pacifico Yokohama, Japan.
6. Kauppinen, E., Lind, T., Kurkela, J., Latva-Somppi, J., Lyyränen, J., Valmari, T.: "Ash formation, transformations and deposition during fluidized bed combustion and gasification, ", *in* LIEKKI 2 Combustion and gasification research programme, technical review 1993-1998, (Ed:s Hupa, M., Matinlinna, J.), Vol 1, p. 639, Åbo Akademis Tryckeri, Åbo, Finland 1998.
7. Zevenhoven, M., Blomquist, J-P., Skrifvars, B-J., Backman, R., Hupa, M: The prediction of behaviour of ashes from five different solid fuels in fluidized bed combustion, *accepted Dec. 1999 for publication in Fuel*.
8. Baxter L.L., "Task 2 . Pollutant emission and deposit formation during combustion of biomass fuels", Quarterly report to National renewable Energy Laboratory, Sandia National Laboratories, Livermore, (CA), USA, 1994.
9. Benson S.A., Holm P.L: Ind. Chem. Eng. Prod. Res. Dev. 24, (1985), 145-149
10. Skrifvars, B-J., Blomquist, J-P., Hupa, M., Backman, R.: Predicting the ash behaviour during biomass combustion in FBC conditions by combining advanced fuel analyses with thermodynamic multicomponent equilibrium calculations, *presented at* the 15th Annual International Pittsburgh Coal Conference, Pittsburgh, PA, USA, September 1998.
11. Peltonen K., Hiltunen, M., Blomquvist, J-P., Skrifvars, B-J., Kurkela, J., Latva-Somppi, J., Kauppinen, E.: Fouling of the cooling surfaces in biofuel-fired fluidized bed boilers, *in proc. of* the ASME 15th FBC Conference, May 1999, Savannah, GA, USA, 1999.
12. Öhman, M.; Nordin, A: Energy & Fuels, 12, (1998), 90-94.
13. Backman, R.: Sodium and sulfur chemistry in combustion gases, Ph. D. Thesis, Åbo Akademi University, 1989.
14. Backman, R.: Melting behavior of salt mixtures in the system (Na, K)(SO_4, CO_3, Cl), Report 94-2, Combustion Chemistry Research Group, Åbo Akademi University 1994.

15. Backman, R., Blomquist, J-P., Ståhlström A.: Ash atlas. Composition of gas and condensed phases of five solid fuels in pressurized combustion and gasification, Report to the participants of the long term durability and reliability if hot ceramic filters, a TEKES project, July 1996..
16. SGTE-database for pure substances, Scientific Group Thermodata Europe, 1994.
17. Pelton, A., Eriksson, G: Proc of the 1st Conf. on Advances in Fusion of Glass, Am.Cer.Soc., (1988), 27.1-29.11.
18. Wu, P., Eriksson, G., Pelton A: J. Am. Ceram.Soc., 76(8), (1993), 2059-2064.
19. Eriksson G., Pelton A: Met Trans. B., 24B (1993), 807-816.
20. Zevenhoven, M., Backman, R: The Chemistry of Biomass Ashes in Pressurised Gasification, Report 98-2, Combustion Chemistry Research Group, Åbo Akademi University, Turku, Finland, 1998.
21. Zevenhoven, M., Backman, R: The Chemistry of Biomass Ashes in Pressurised Gasification Part II, Report 99-2, Combustion Chemistry Research Group, Åbo Akademi University, Turku, Finland, 1999.
22. Zevenhoven, M., Laurén, T., Skrifvars, B-J., Backman, R: The chemistry and melting behaviour of fly ash deposits in co-combustion of green liquor sludge and spruce bark, Report 99-10, Combustion Chemistry Research Group, Åbo Akademi University, Turku, Finland, 1999.
23. Morey, G.W., Kracek, F.C., Bowen, N.L J: Soc. Glass Technol., 14, (1930), 158.

APPENDIX, Figures

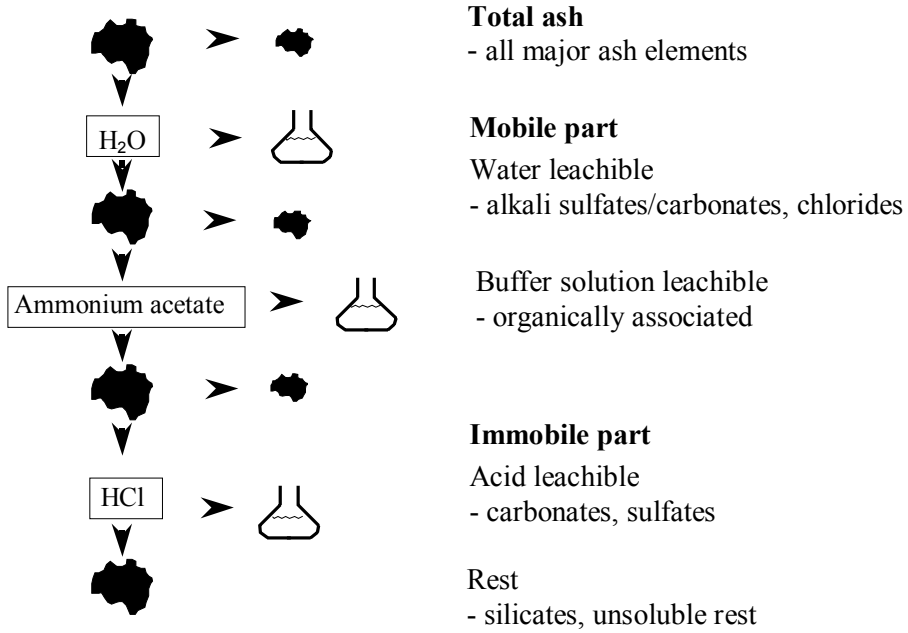

Figure 1. A schematic view of the Chemical fractionation analysis technique, such as it was developed for coals /8, 9/
Figur 1. En schematisk översikt av den Kemiska fraktionerings tekniken, såsom den utveckladed för kol /8, 9/

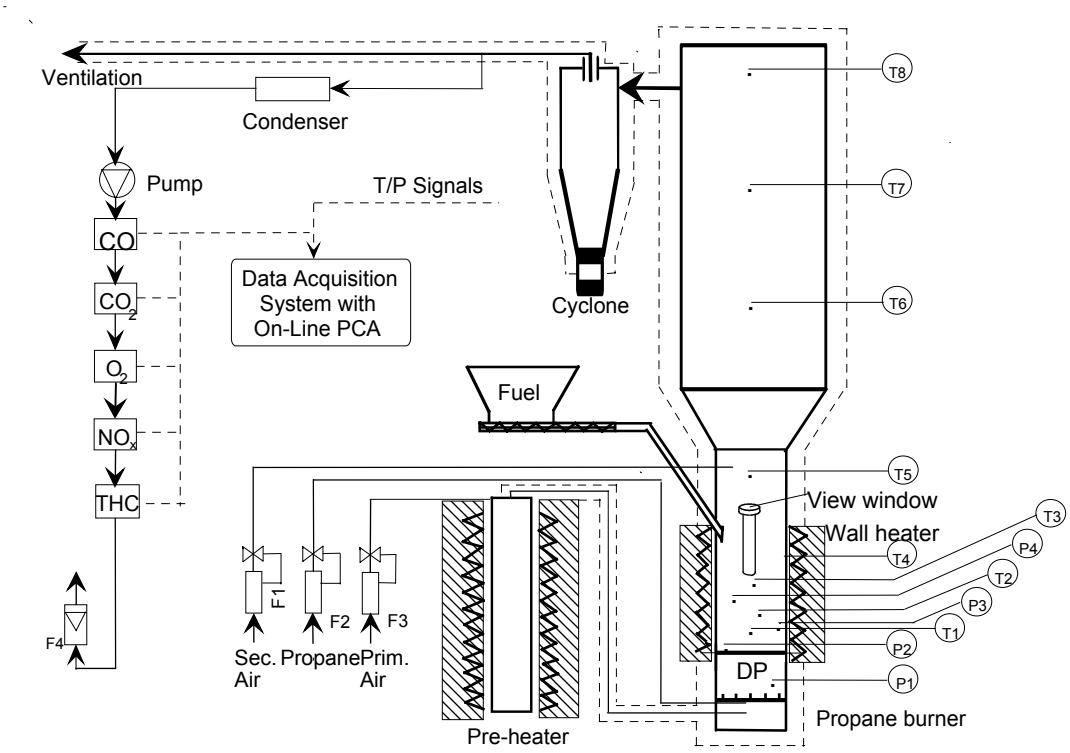

Figure 2. Illustration of the bench scale fluidized bed reactor /2/.
Figur 2. Schematisk bild över pilotreaktorn /2/.

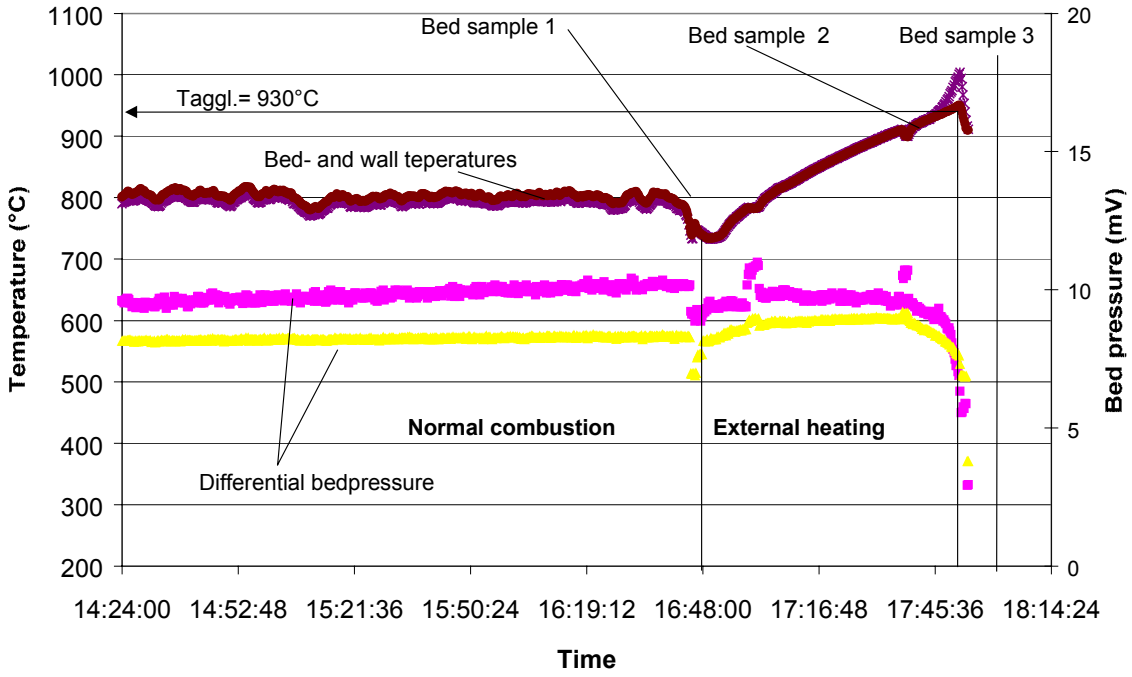

Figure 3. A typical agglomeration test run, in this case with Bark.
Figur 3. Exempel på kontrollerat agglomereringsförsök på Bark.

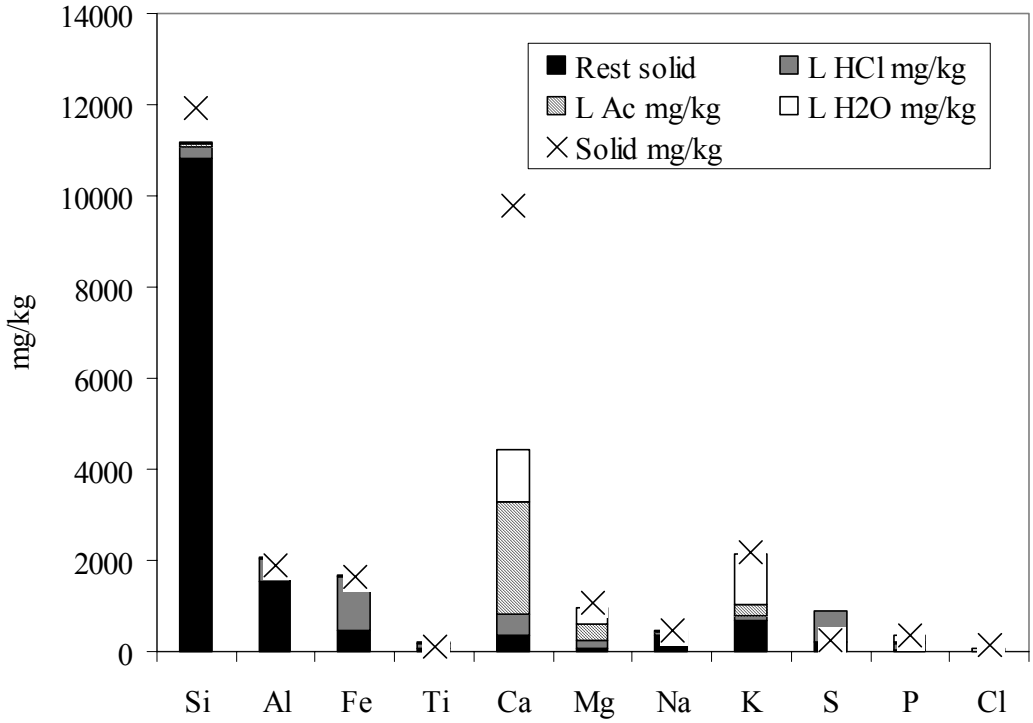

Figure 4a. The absolute amounts of ash forming elements in the dry bark distributed in the four different fractions.

Figur 4a. Absoluta mängder av askbildande elementen i torr bark, distribuerade i de fyra olika fraktionerna

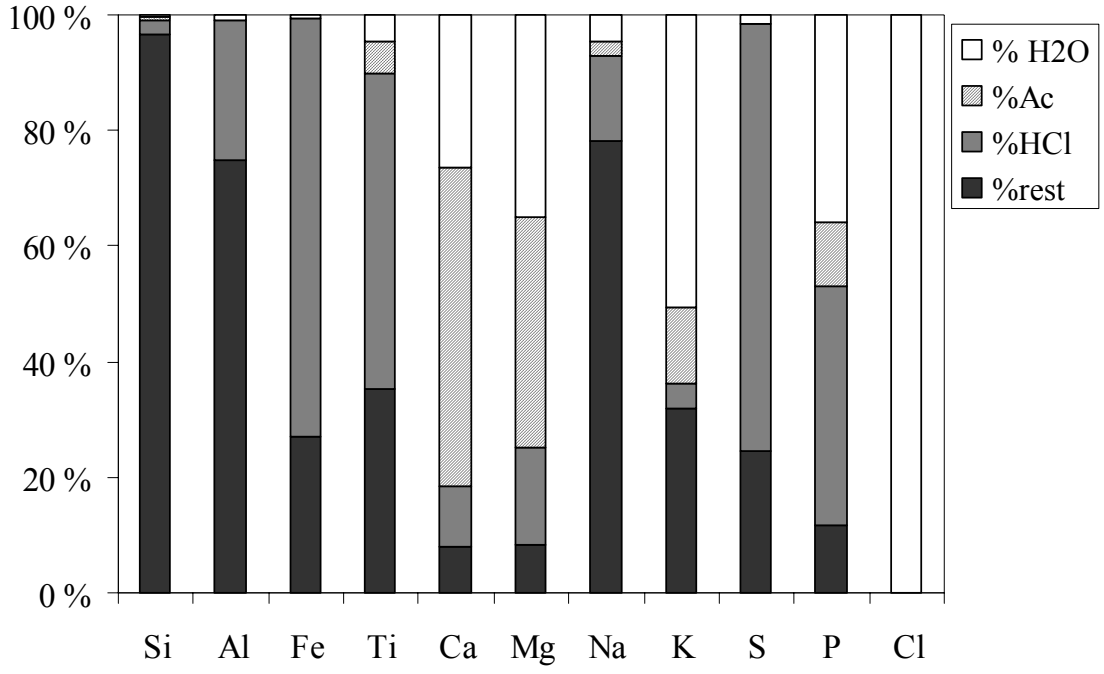

Figure 4b. The distribution of ash forming elements in the four different fractions of the dry bark, on a percentage base

Figur 4b. Den procentuella fördelningen av askbildande element i bark, distribuerade i de fyra olika fraktionerna

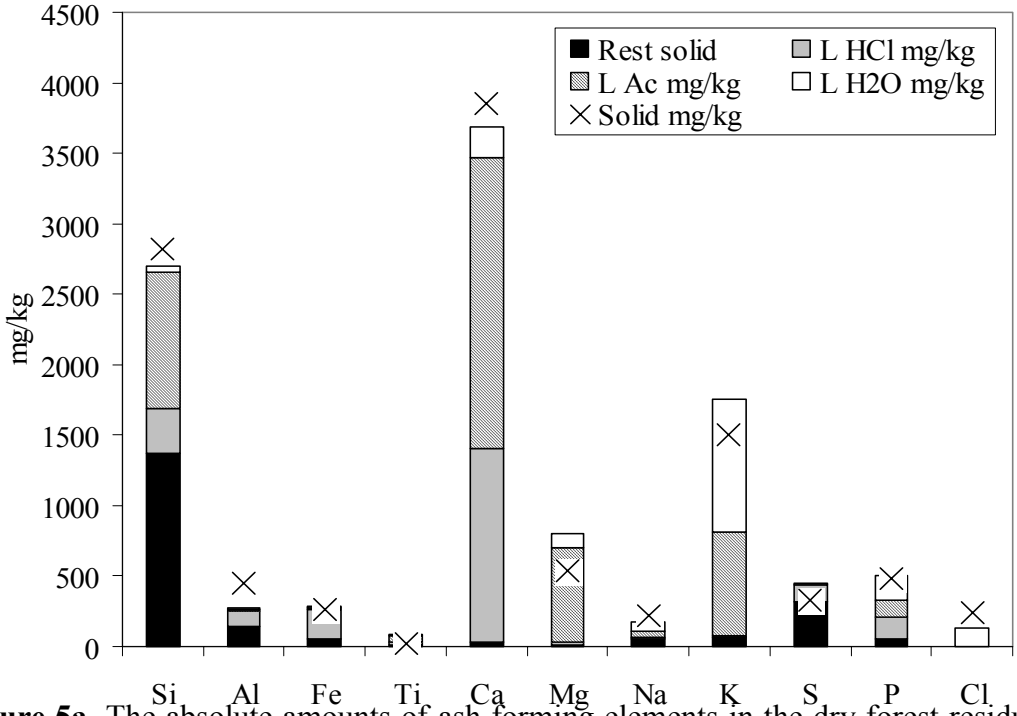

Figure 5a. The absolute amounts of ash forming elements in the dry forest residue type 1, distributed in the four different fractions.

Figur 5a. Absoluta mängder av askbildande elementen i torr skogsflis, typ 1 (brun grot), distribuerade i de fyra olika fraktionerna

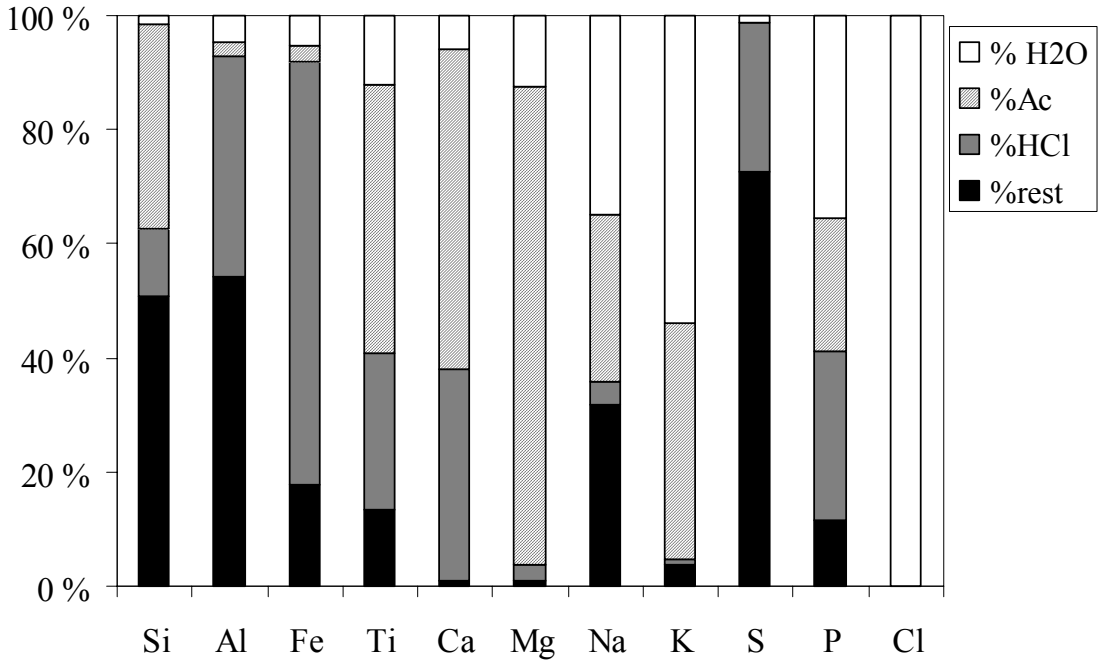

Figure 5b. The distribution of ash forming elements in the four different fractions of the forest residue type 1, on a percentage base

Figur 5b. Den procentuella fördelningen av askbildande element i skogsflis typ 1 (brun grot), distribuerade i de fyra olika fraktionerna

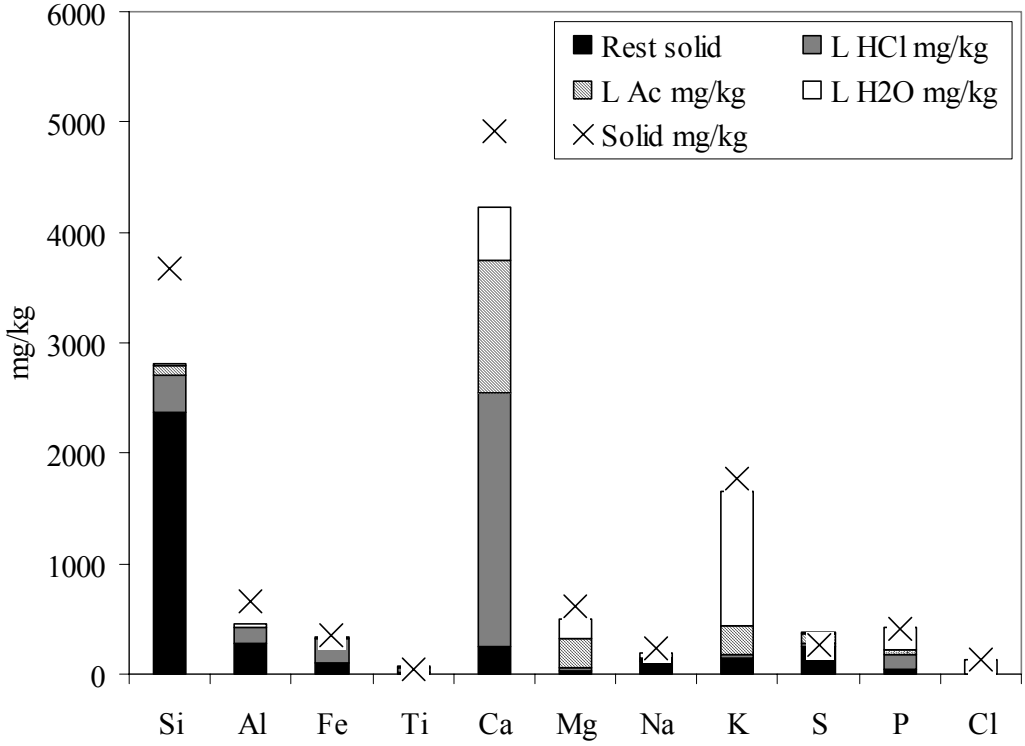

Figure 6a. The absolute amounts of ash forming elements in the dry forest residue type 2, distributed in the four different fractions.
Figur 6a. Absoluta mängder av askbildande elementen i torr skogsflis, typ 2 (grön grot), distribuerade i de fyra olika fraktionerna

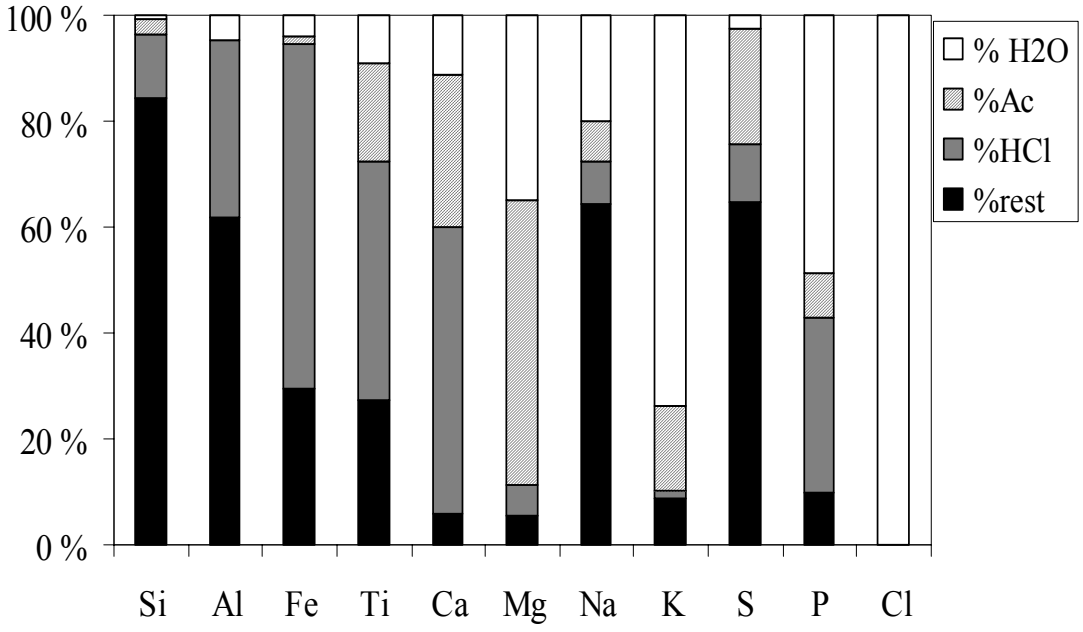

Figure 6b. The distribution of ash forming elements in the four different fractions of the forest residue type 2, on a percentage base
Figur 6b. Den procentuella fördelningen av askbildande element i skogsflis typ 2 (grön grot), distribuerade i de fyra olika fraktionerna

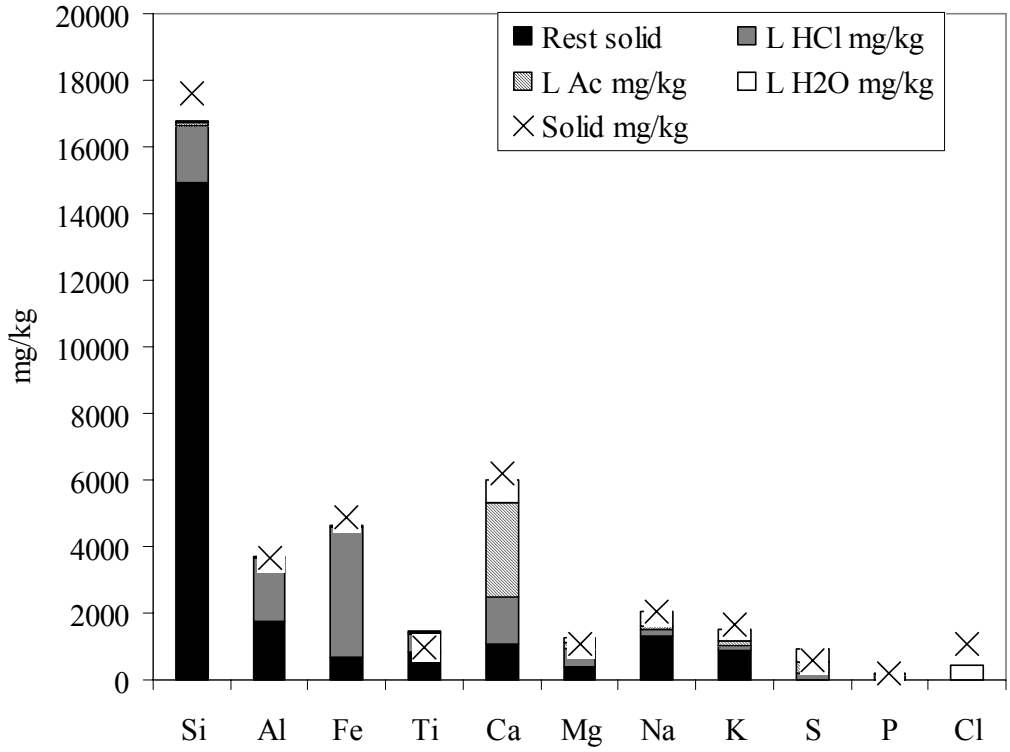

Figure 7a. The absolute amounts of ash forming elements in the dry construction residue, distributed in the four different fractions.

Figur 7a. Absoluta mängder av askbildande elementen i torr returflis, distribuerade i de fyra olika fraktionerna

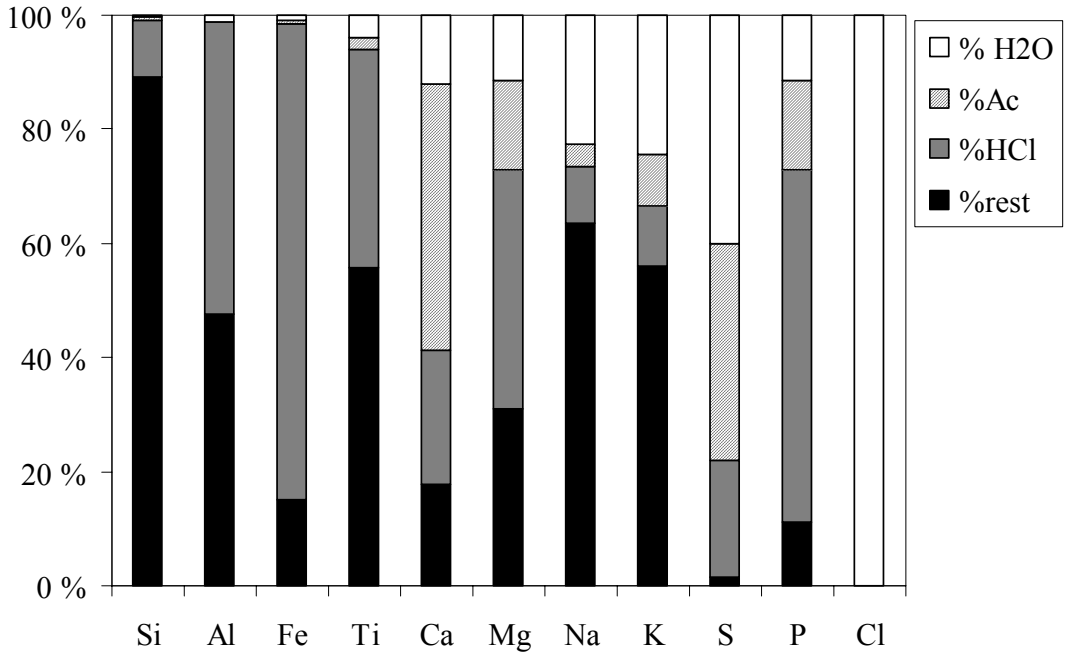

Figure 7b. The distribution of ash forming elements in the four different fractions of the construction residue, on a percentage base

Figur 7b. Den procentuella fördelningen av askbildande element i returflis, distribuerade i de fyra olika fraktionerna

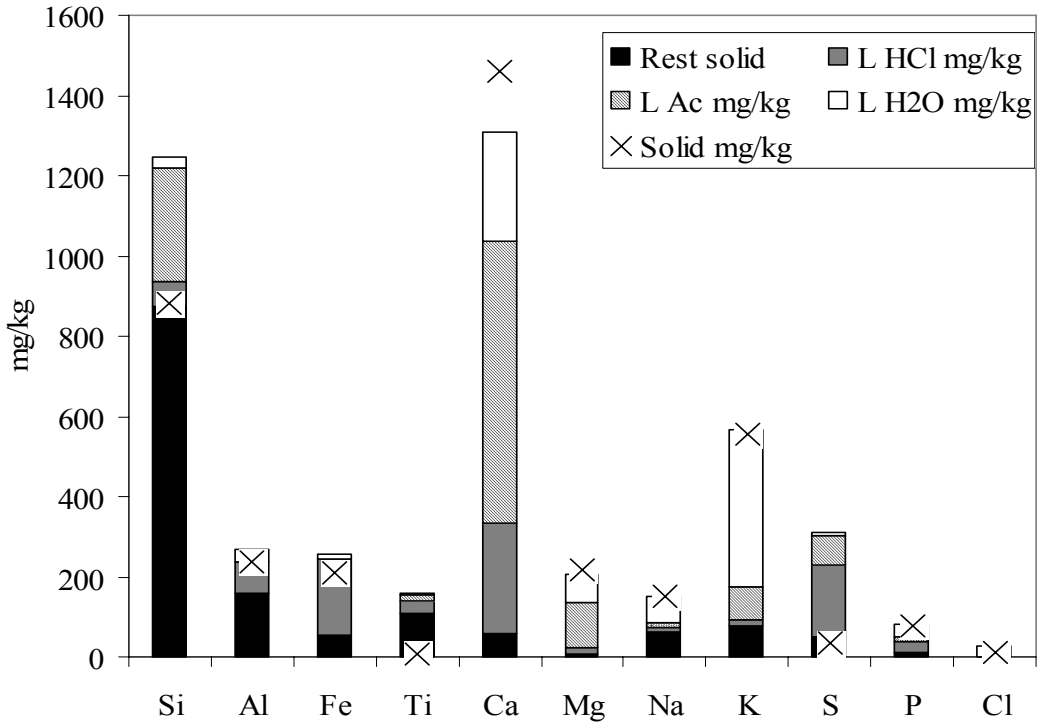

Figure 8a. The absolute amounts of ash forming elements in the dry sawdust, distributed in the four different fractions.
Figur 8a. Absoluta mängder av askbildande elementen i torrt sågspån (trä), distribuerade i de fyra olika fraktionerna

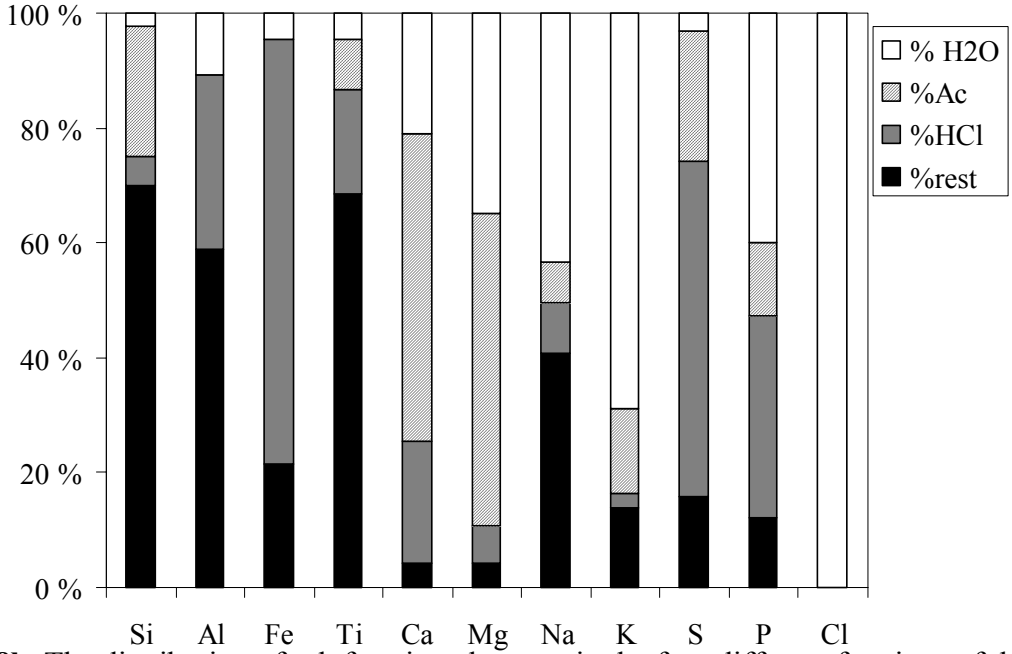

Figure 8b. The distribution of ash forming elements in the four different fractions of the saw dust, on a percentage base
Figur 8b. Den procentuella fördelningen av askbildande element i sågspån (trä), distribuerade i de fyra olika fraktionerna.

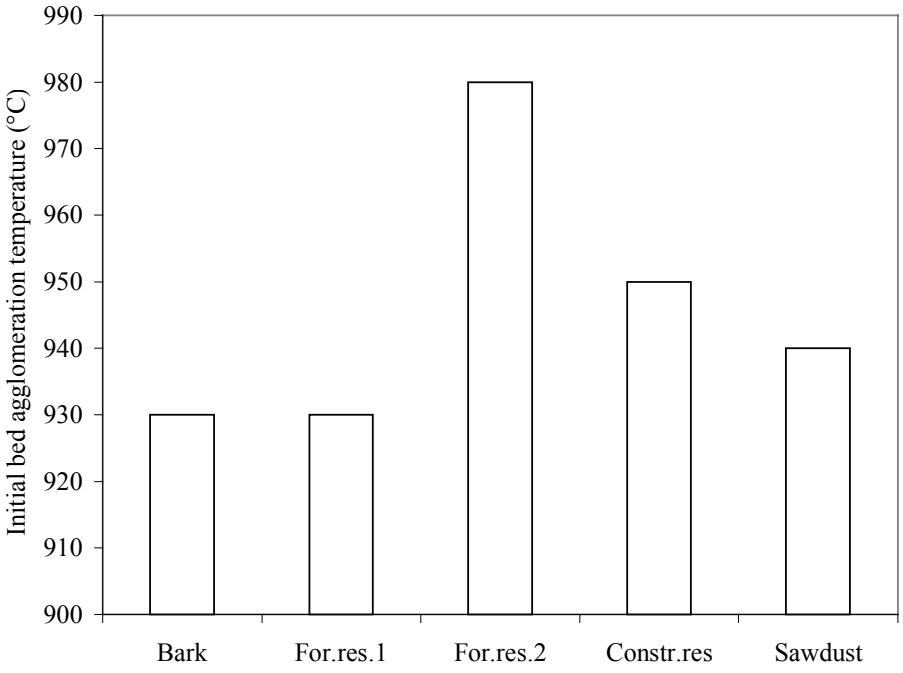

Figure 9. Initial bed agglomeration temperatures
Figur 9. Initiala agglomereringstemperaturer

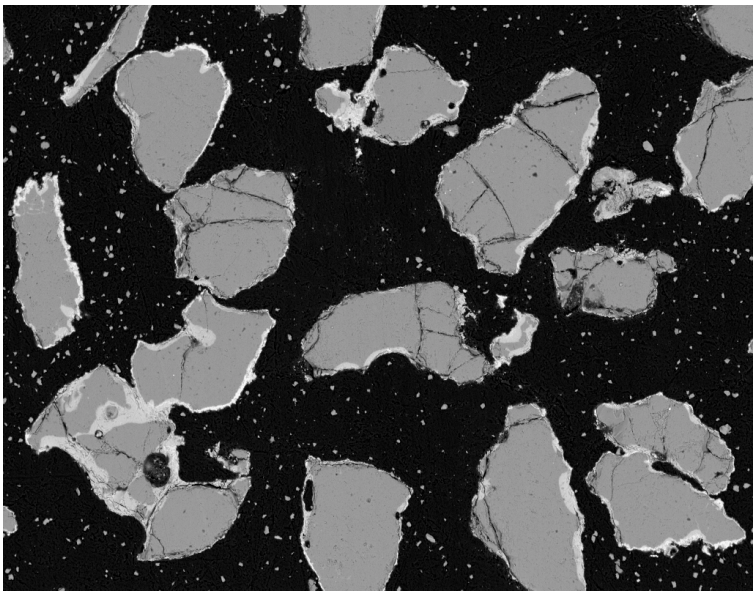

Figure 10. SEM pictures (back scatter image) of bed particles and agglomerates from the controlled bed agglomeration test of sawdust. Magnification x120
Figur 10. SEM bild (back scatter) av bäddpartiklar och agglomerat från det kontrollerade bäddagglomereringsförsöket för sågavfall. Förstoring x120.

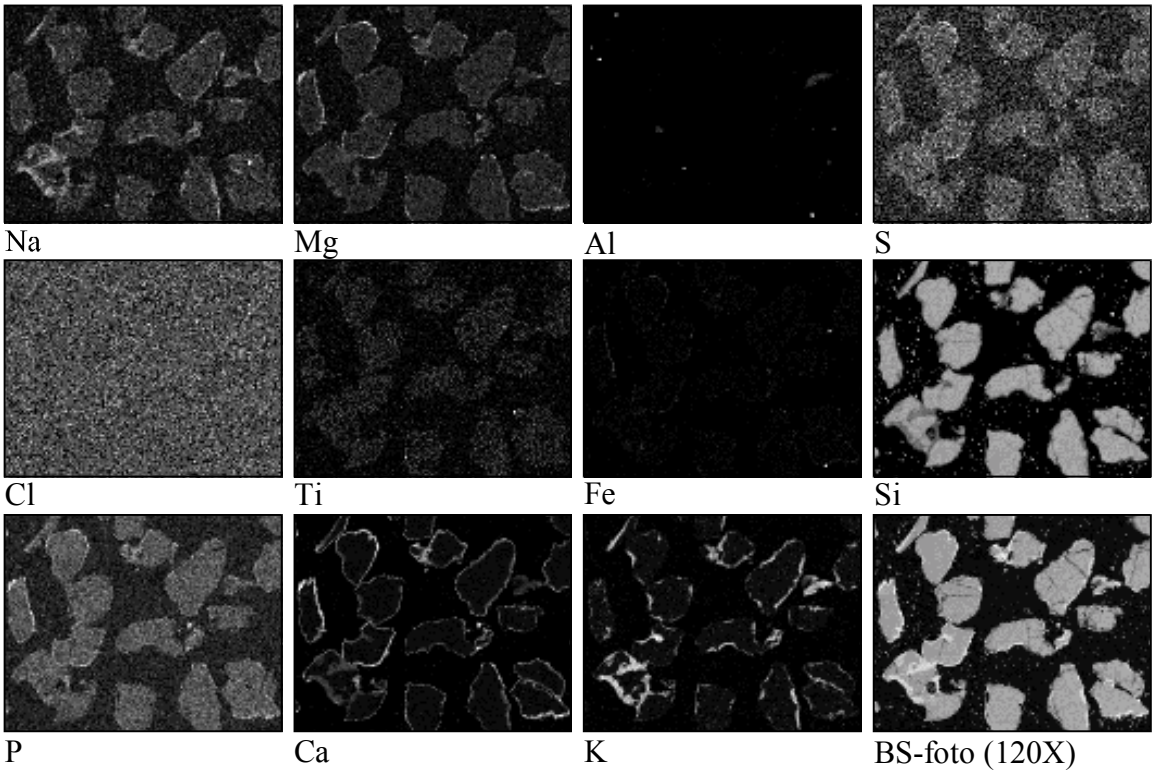

Figure 11. SEM/EDS elemental maps of the elements Na, Mg, Al, S, Cl, Ti, Fe, Si, P, Ca and K in the bed sample taken from the controlled bed agglomeration test of sawdust. (same back scatter image in the lower right corner as in Figure 11)
Figur 11. SEM/EDS elementkartor av elementen Na, Mg, Al, S, Cl, Ti, Fe, Si, P, Ca och K i bäddprovet taget från det kontrollerade bäddagglomereringstestet av sågavfall. (samma back scatter image i det lägre högra hörnet zom i Figur 11)

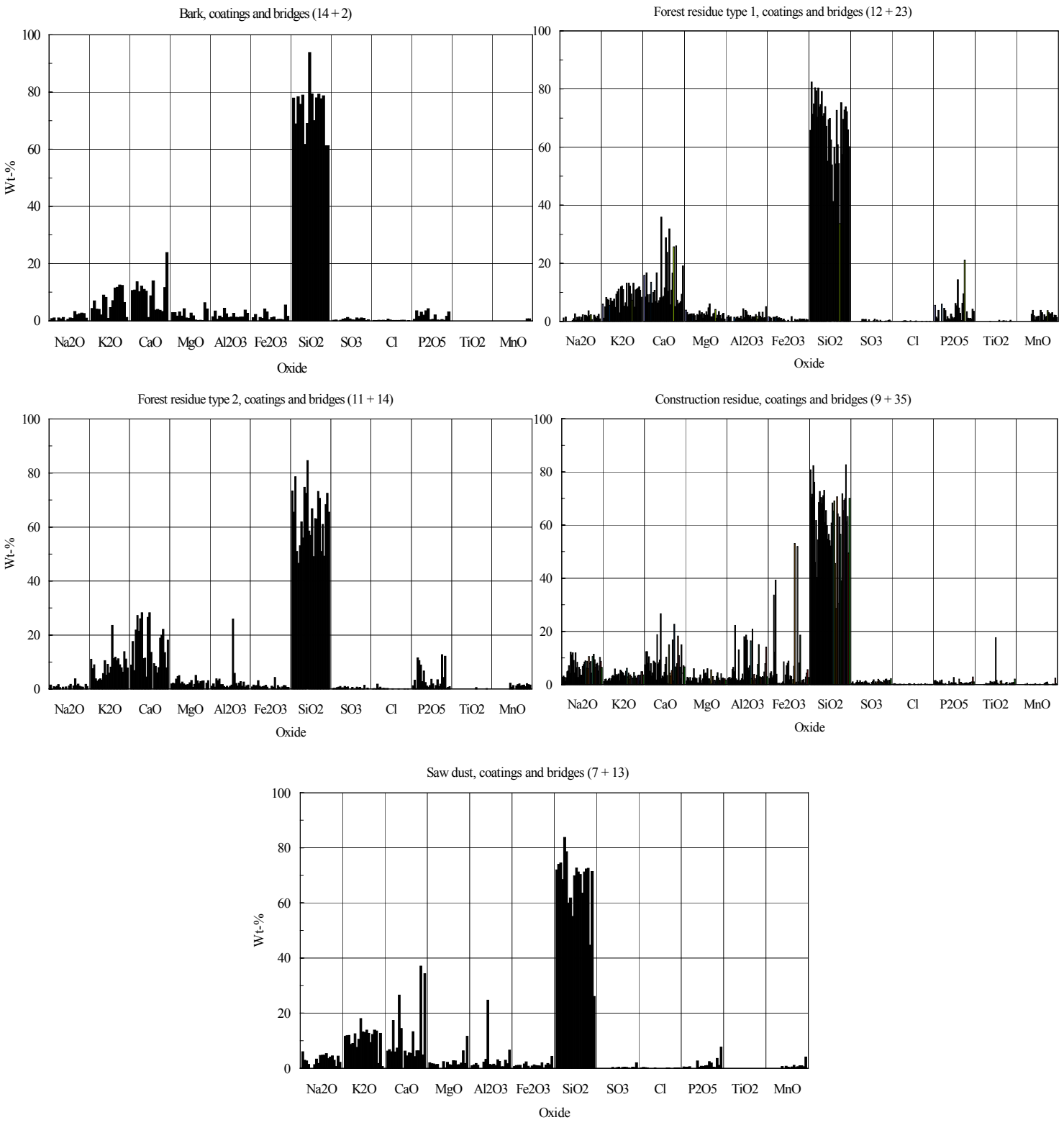

Figure 12. Semi-quantitative SEM/EDS analyses of the composition of bed particle coatings from the controlled bed agglomeration tests of the five fuels.
Figur 12. Semi-kvantitativa SEM/EDS analyser av bäddpartikelskalens sammansättning. Bäddproven tagna från de kontrollerade bäddagglomereringstesten för de 5 testbränslena.

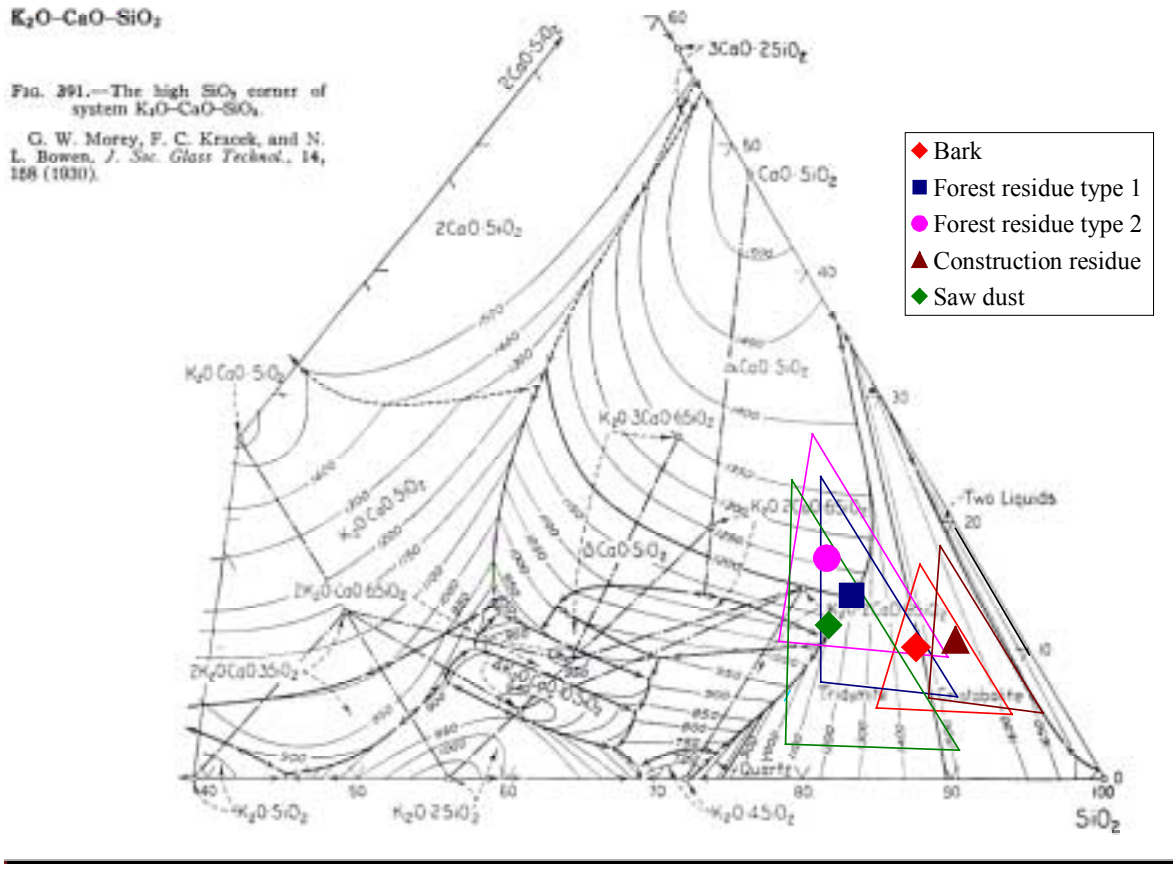

Figure 13. The average compositions of the bed particle coatings from the 5 test fuels, plotted in the 3-phase diagram K_2O-CaO-SiO_2. The triangel around each dot indicates the scattering of the analysed compositions.

Figur 13. Medelsammansättningen av bäddpartikelskalen från de kontrollerade agglomereringstesten för de 5 testbränslena, inritade i 3-fasdiagrammet K_2O-CaO-SiO_2. Trianglarna runt varje punkt indikerar spridningen på analyserna.

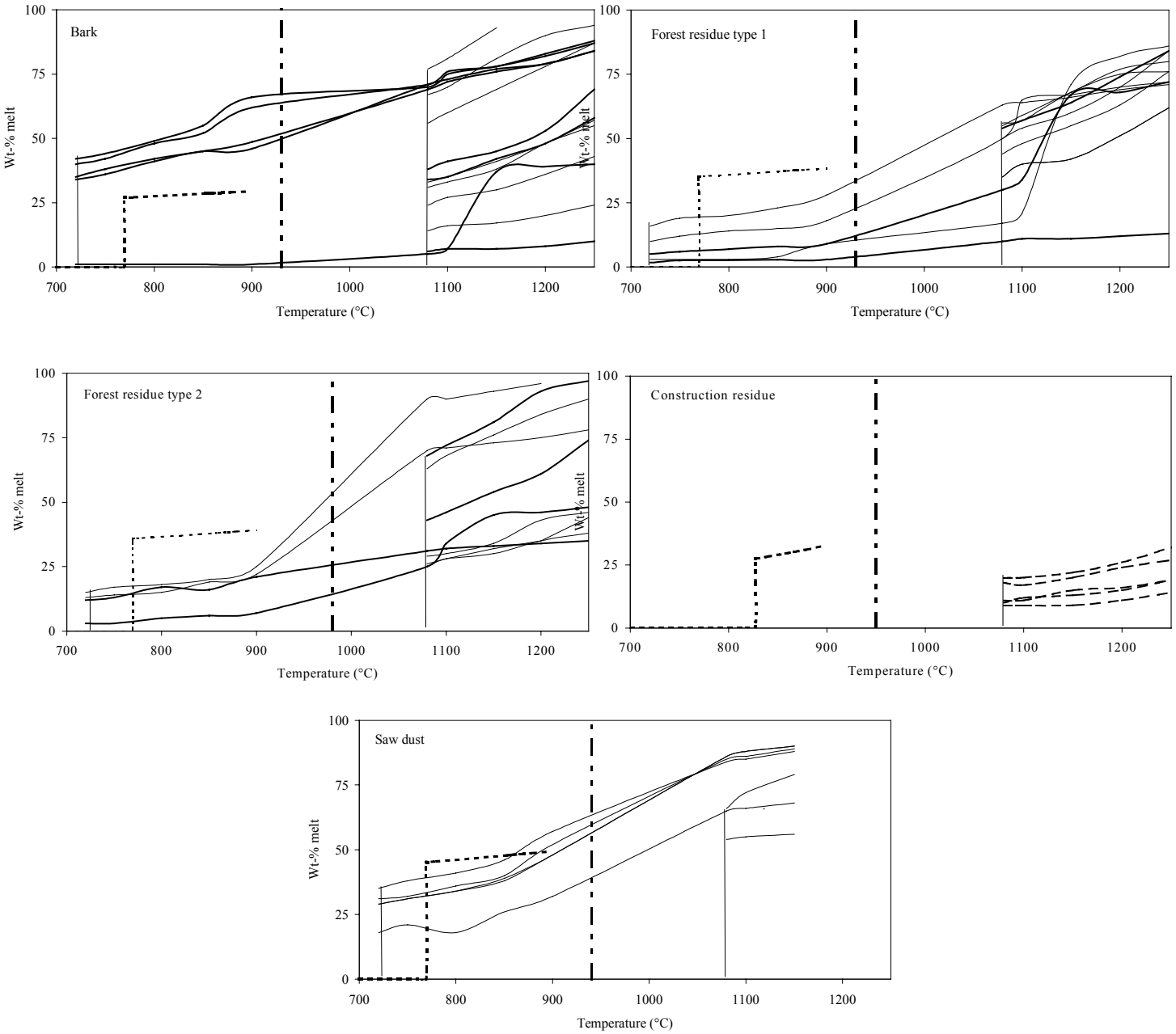

Figure 14. Estimated (solid lines) and calculated (dotted line) amount of molten phase in the coating of the bed particle from the controlled bed agglomeration test of the 5 test fuels. Each solid line represents a spot analysis in the coating. The dotted line represents a calculated amount where the input values have been the average composition of the coating presented in Figure 13. The vertical line represents the measured bed agglomeration temperature.

Figur 14. Estimerade (heldragna linjerna) och beräknade (punkterade linjen) mängder smälta i bäddpartikelskalen från de kontrollerade bäddagglomereringstesten av de 5 testbränslena. Varje heldragen linje representerar en punktanalys i skalet. Den punkterade linjen representerar den beräknade mängden smälta utgående från medelsammansättningen på skalet presenterat i Figur 13. Den lodräta line representerar den uppmätta bäddagglomereringstemperaturen.

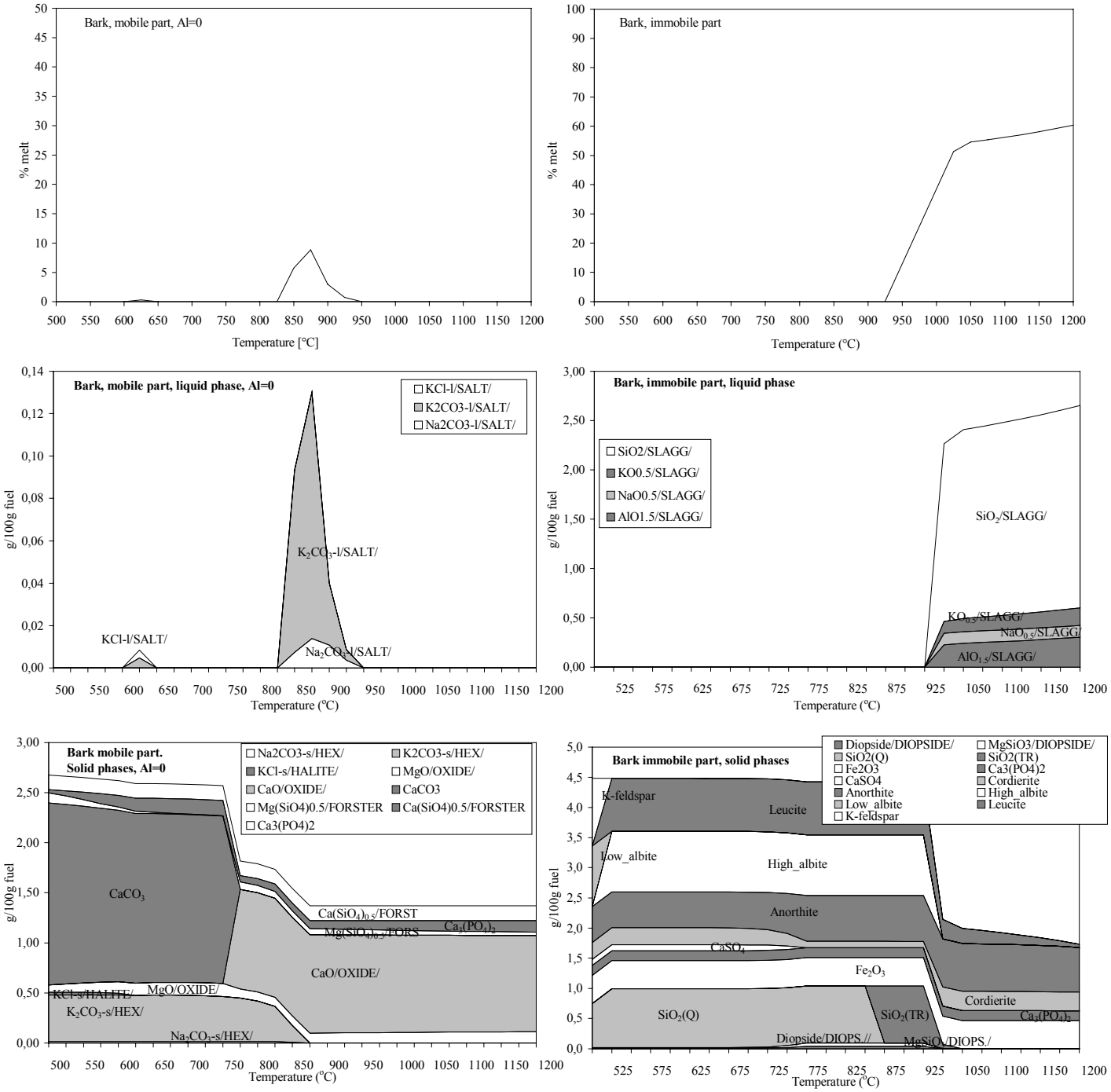

Figure 15. The results from the global equilibrium analyses of the two parts of ash particle fractions in Bark, estimated from the chemical fractionation analyses. 1) Mobile part (left column). 2) Immobile part (right column).Top: The amount of molten phase in each part. Middle: The composition of the molten phase in each part. Down: The solid phases in each part.

Figur 15. Resultaten av den globala jämviktsanalysen av de två askpartikelfraktionerna i Bark, uppskattade på basen av den kemiska fraktioneringsanalysen. 1) Den mobila fraktionen (vänstra kolumnen). 2) Den immobila fraktionen (högra kolumnen). Överst: Andelen smälta i vardera fraktionen. Mitten: Den smälta fasens sammansättning i vardera fraktionen. Nederst: De fasta faserna i vardera fraktionen.

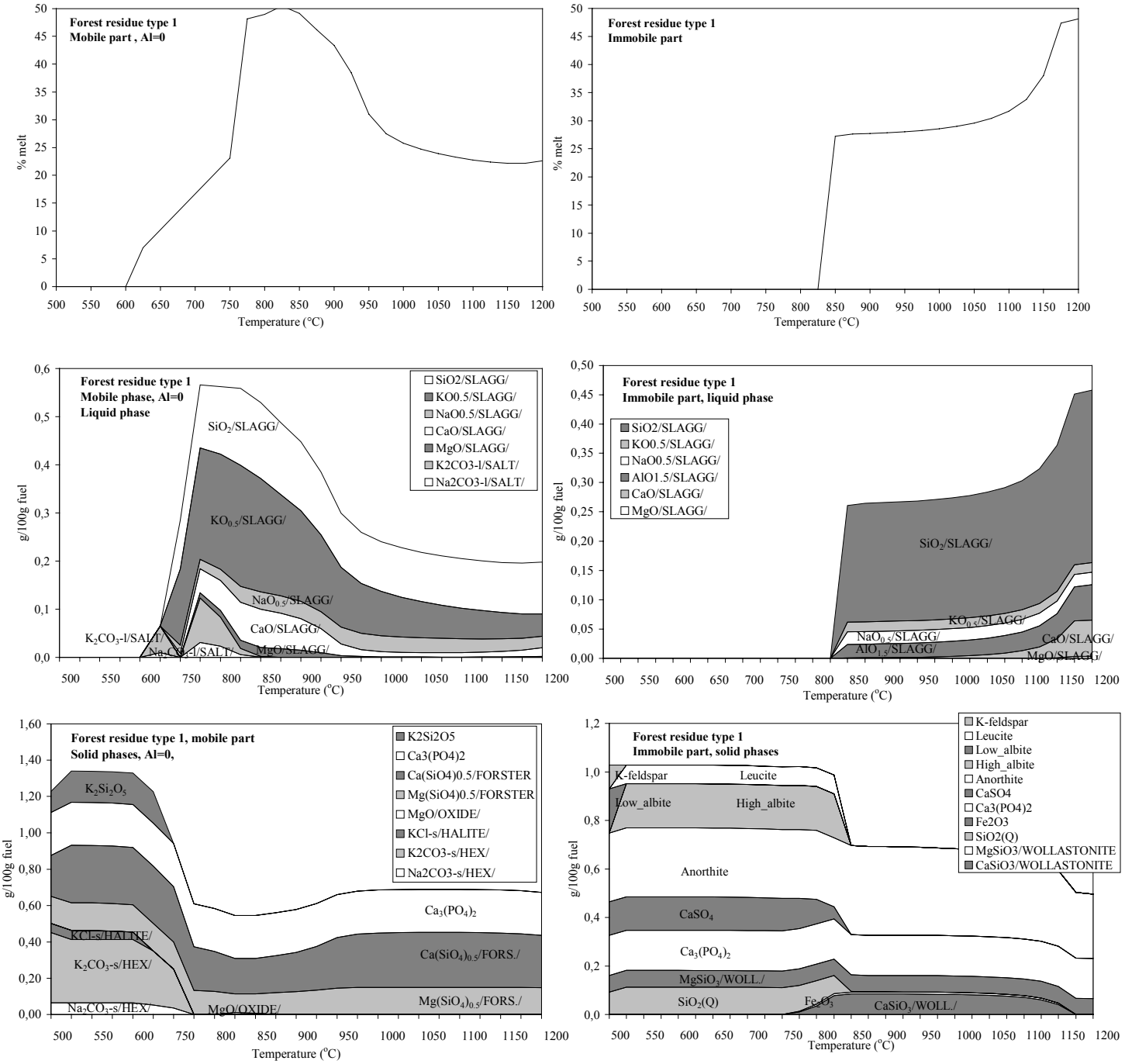

Figure 16. The results from the global equilibrium analyses of the two parts of ash particle fractions in Forest residue type 1, estimated from the chemical fractionation analyses. 1) Mobile part (left column). 2) Immobile part (right column).Top: The amount of molten phase in each part. Middle: The composition of the molten phase in each part. Down: The solid phases in each part.

Figur 16. Resultaten av den globala jämviktsanalysen av de två askpartikelfraktionerna i Brun grot, uppskattade på basen av den kemiska fraktioneringsanalysen. 1) Den mobila fraktionen (vänstra kolumnen). 2) Den immobila fraktionen (högra kolumnen). Överst: Andelen smälta i vardera fraktionen. Mitten: Den smälta fasens sammansättning i vardera fraktionen. Nederst: De fasta faserna i vardera fraktionen.

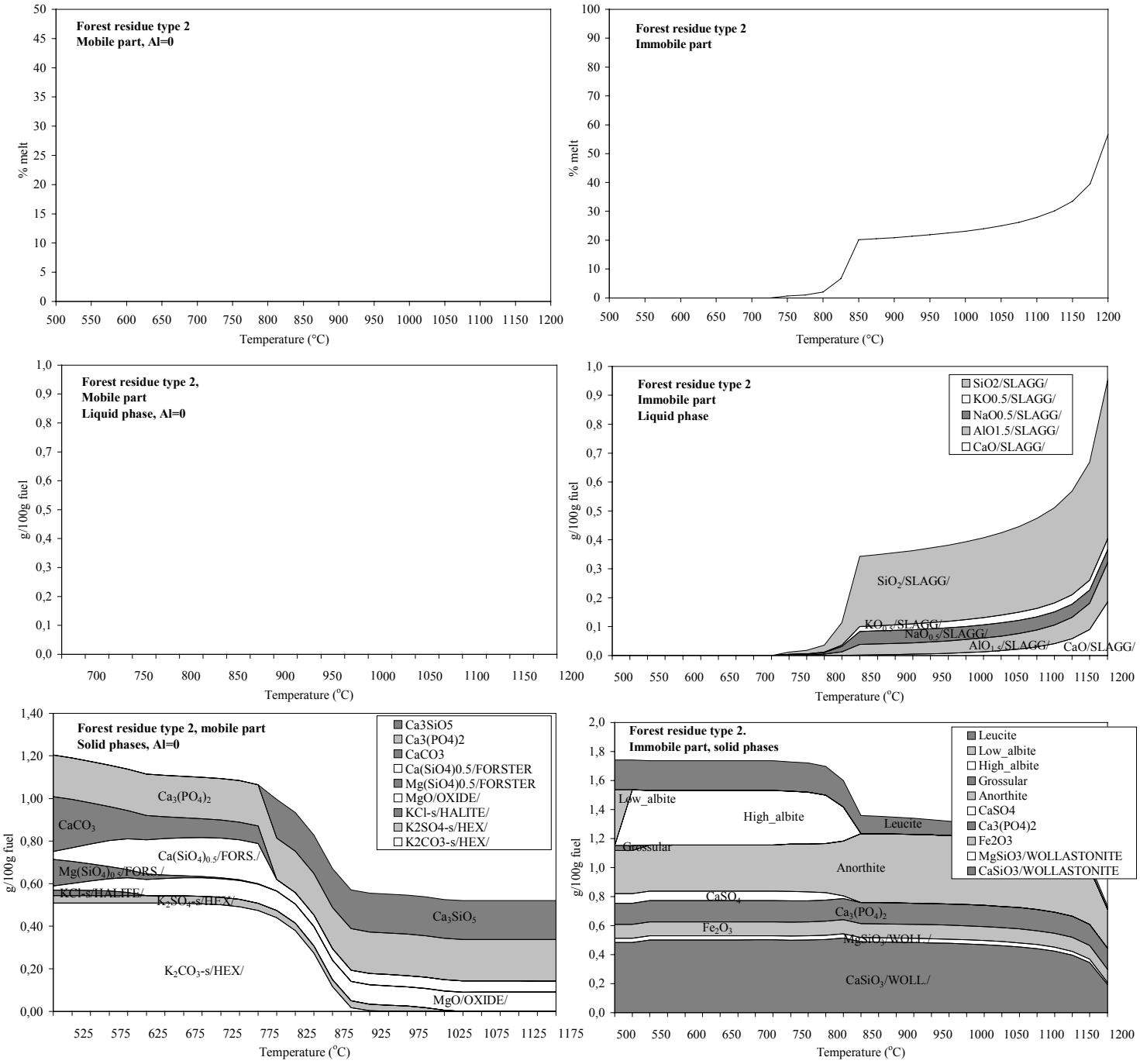

Figure 17. The results from the global equilibrium analyses of the two parts of ash particle fractions in Forest residue type 2, estimated from the chemical fractionation analyses. 1) Mobile part (left column). 2) Immobile part (right column).Top: The amount of molten phase in each part. Middle: The composition of the molten phase in each part. Down: The solid phases in each part.

Figur 17. Resultaten av den globala jämviktsanalysen av de två askpartikelfraktionerna i Grön grot, uppskattade på basen av den kemiska fraktioneringsanalysen. 1) Den mobila fraktionen (vänstra kolumnen). 2) Den immobila fraktionen (högra kolumnen). Överst: Andelen smälta i vardera fraktionen. Mitten: Den smälta fasens sammansättning i vardera fraktionen. Nederst: De fasta faserna i vardera fraktionen.

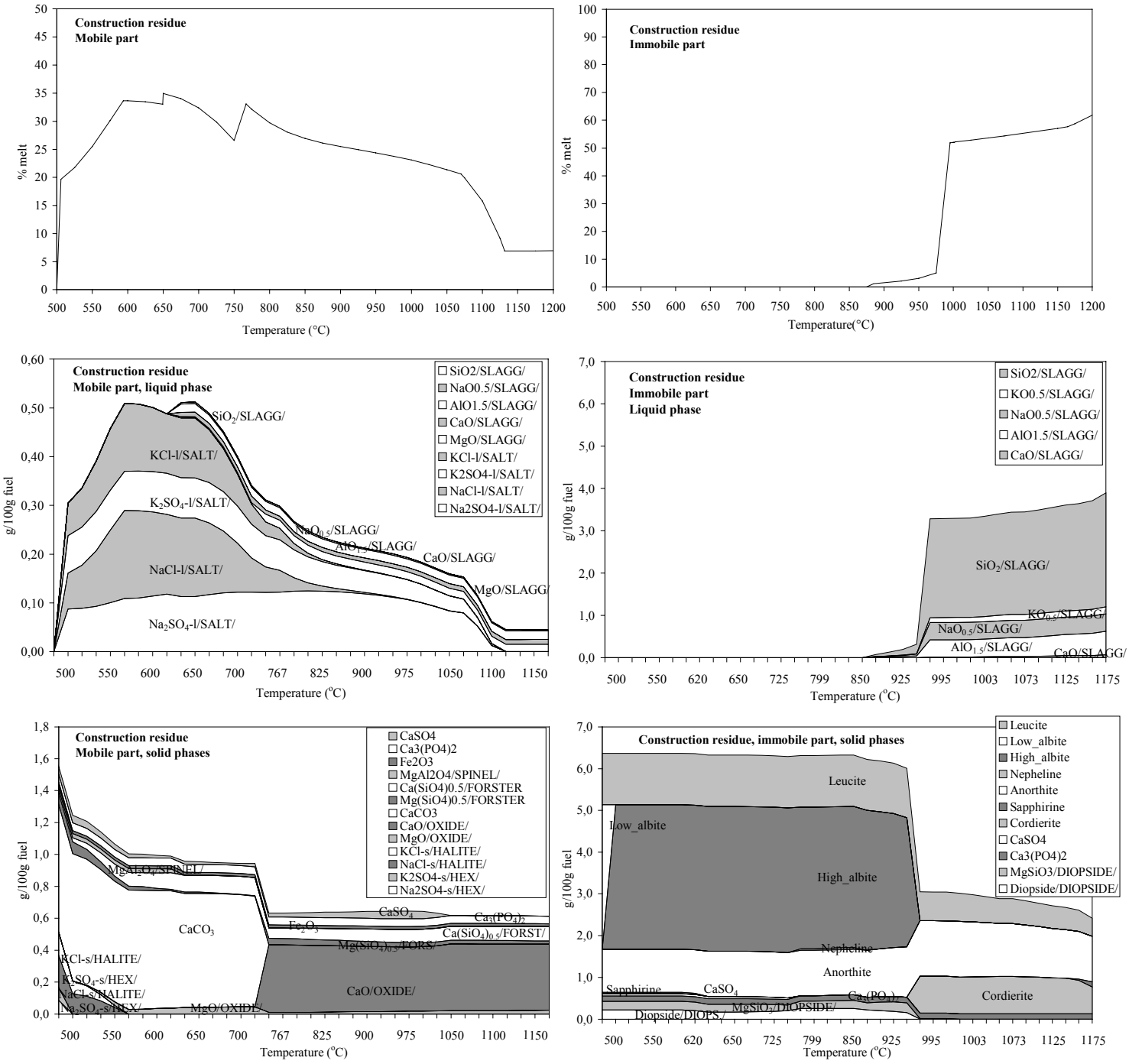

Figure 18. The results from the global equilibrium analyses of the two parts of ash particle fractions in Construction residue, estimated from the chemical fractionation analyses. 1) Mobile part (left column). 2) Immobile part (right column).Top: The amount of molten phase in each part. Middle: The composition of the molten phase in each part. Down: The solid phases in each part.

Figur 18. Resultaten av den globala jämviktsanalysen av de två askpartikelfraktionerna i Returflis, uppskattade på basen av den kemiska fraktioneringsanalysen. 1) Den mobila fraktionen (vänstra kolumnen). 2) Den immobila fraktionen (högra kolumnen). Överst: Andelen smälta i vardera fraktionen. Mitten: Den smälta fasens sammansättning i vardera fraktionen. Nederst: De fasta faserna i vardera fraktionen.

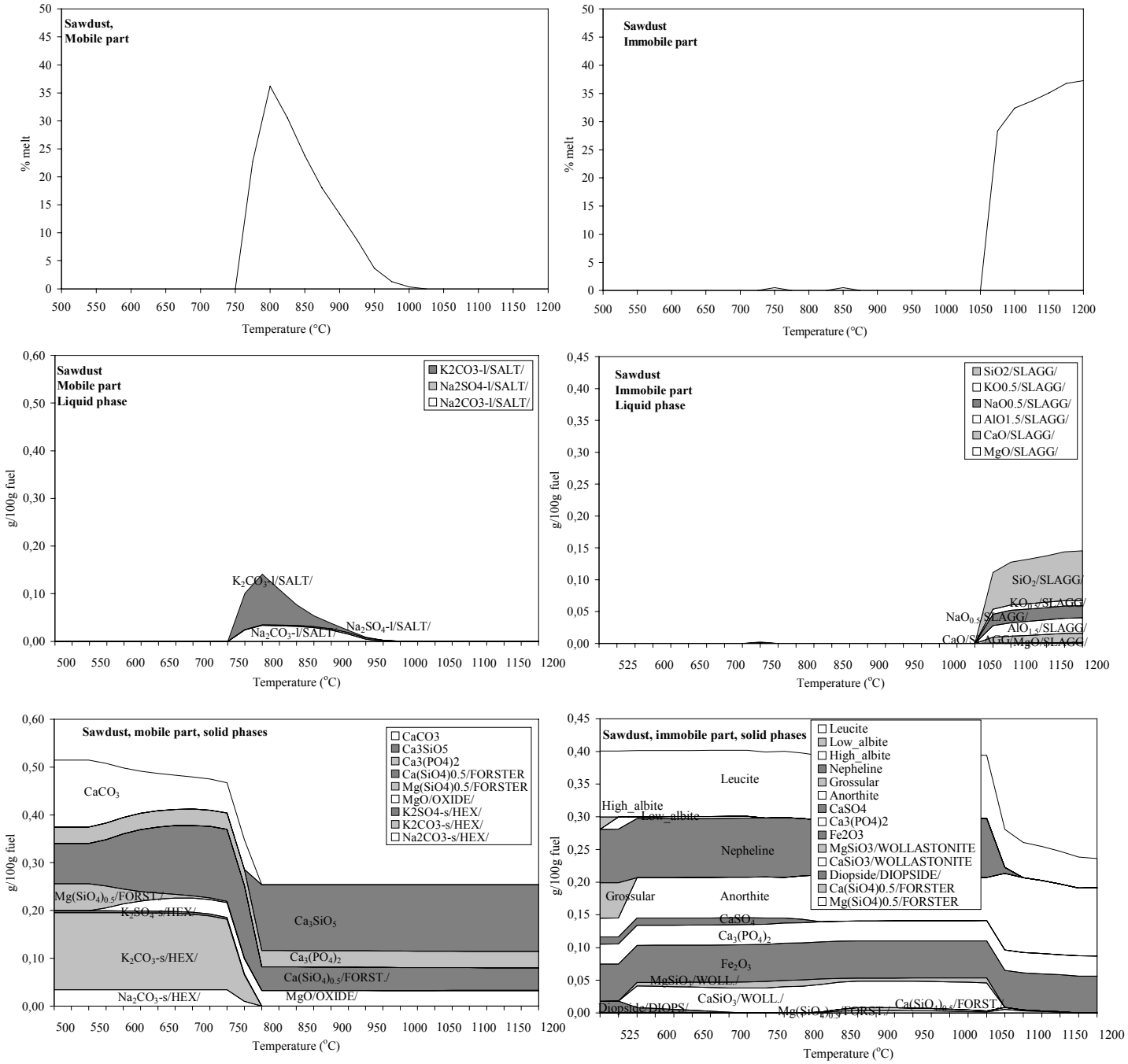

Figure 19. The results from the global equilibrium analyses of the two parts of ash particle fractions in Sawdust, estimated from the chemical fractionation analyses. 1) Mobile part (left column). 2) Immobile part (right column).Top: The amount of molten phase in each part. Middle: The composition of the molten phase in each part. Down: The solid phases in each part.

Figur 19. Resultaten av den globala jämviktsanalysen av de två askpartikelfraktionerna i Sågavfall , uppskattade på basen av den kemiska fraktioneringsanalysen. 1) Den mobila fraktionen (vänstra kolumnen). 2) Den immobila fraktionen (högra kolumnen). Överst: Andelen smälta i vardera fraktionen. Mitten: Den smälta fasens sammansättning i vardera fraktionen. Nederst: De fasta faserna i vardera fraktionen.

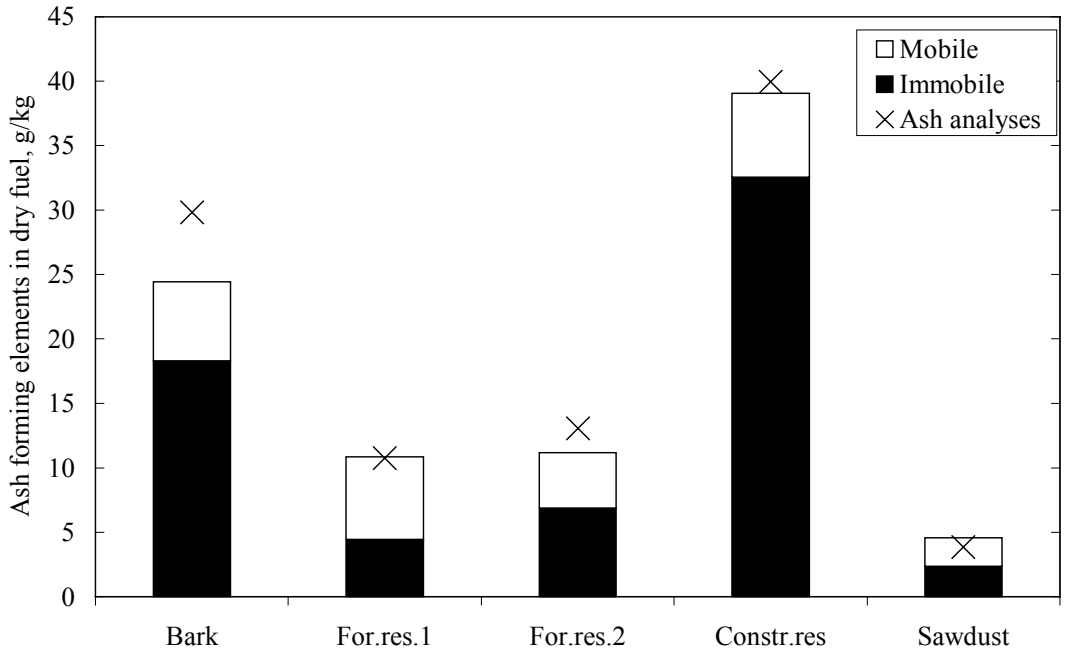

Figure 20. The sum of ash forming elements in the mobile and immobile parts of each fuel as they were analyzed with the chemical fractionation analysis. The cross at each bar indicates the analysed amount of ash, recalculated to elements in the dry fuel.
Figur 20. Summan av askbildande element i den mobila och den immobila delen av varje bränsle såsom de analyserades med den kemiska fraktioneringsanalysen. Krysset vid varje stapel indikerar den totala mängden aska analyserat i varje bränsle, omräknat till element i torrt bränsle.

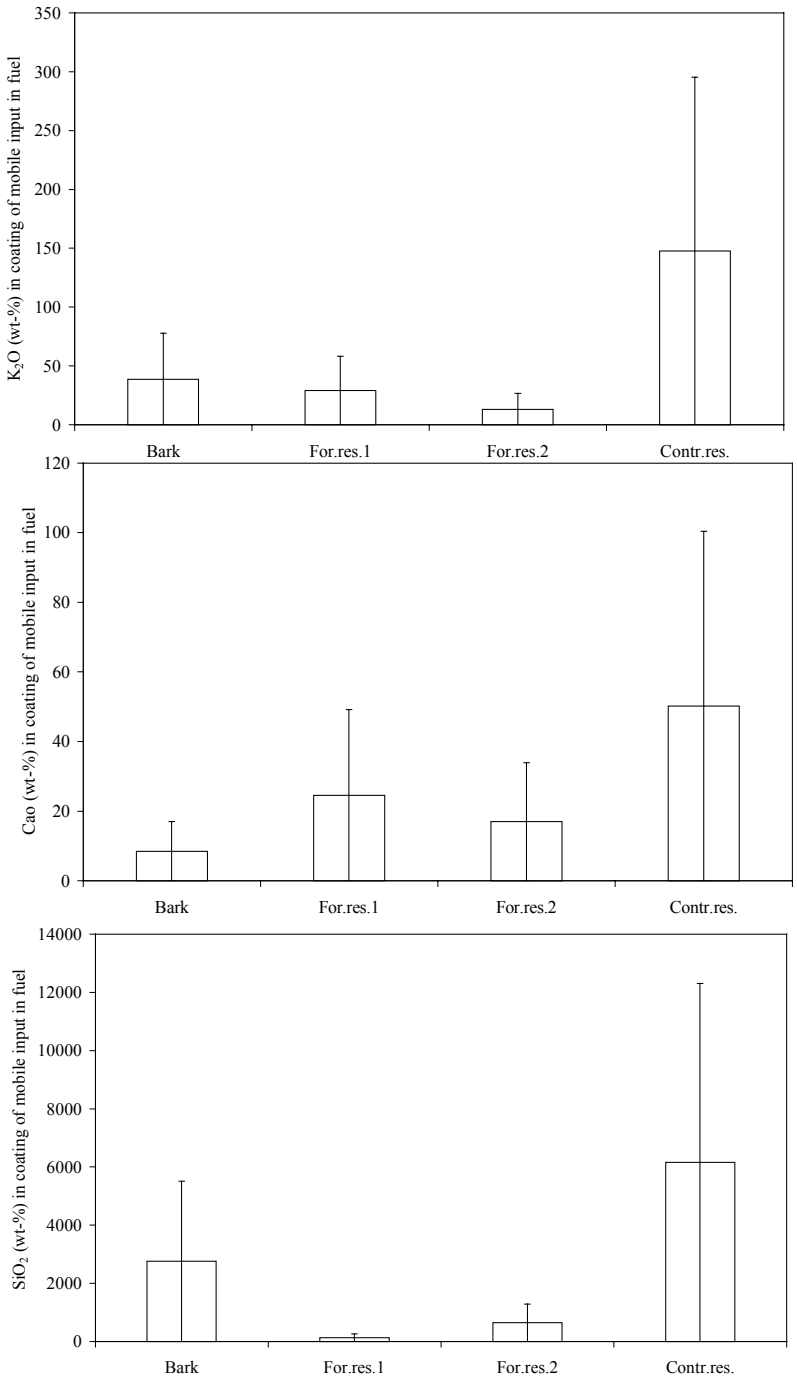

Figure 21. An estimation of the source to the elements potassium (K), calcium (Ca) and silicon (Si), found in the coatings. The estimation is based on the analyses of the element in question from the easily volatilized ash part in the fuel and the coating of the bed particle. The vertical bar indicates the scattering of the results originating from the estimated bed loss.

Figur 21. En uppskattning av källan till kalium (K), kalcium (Ca) och kisel (Si) i bäddpartikelskalet. Uppskattningen baserad på den kemiska fraktioneringsanalysens lättlösliga fraktioner och SEM/EDS analysen av bäddpartikelskalet för motsvarande bränsle. Spridningen i uppskattningen anges som det vertikala sträcket vid varje stapel, och hänrör sig från uppskattad bäddförlust.

Värmeforsk är ett organ för industrisamverkan inom värmeteknisk forskning och utveckling. Forskningsprogrammet är tillämpningsinriktat och fokuseras på energi- och processindustriernas behov och problem. Bakom Värmeforsk står följande huvudmän:

- Elforsk
- Svenska Fjärrvärmeföreningen
- Skogsindustrierna
- Övrig Industri

Värmeforsk samarbetar med Statens Energimyndighet.

VÄRMEFORSK Service AB

101 53 Stockholm
Tel 08-677 25 80 ● Fax 08-677 25 35
http://www.varmeforsk.se